

**STUDY OF THREE DIMENSIONAL
COMPOSITES PRINTING MATERIAL
THROUGH SIMULATION**

OWI CHUN KIT

UNIVERSITI TUNKU ABDUL RAHMAN

**STUDY OF THREE DIMENSIONAL COMPOSITE PRINTING
MATERIAL THROUGH SIMULATION**

OWI CHUN KIT

**A project report submitted in partial fulfilment of the
requirements for the award of Bachelor of Engineering
(Honours) Mechanical Engineering**

**Lee Kong Chian Faculty of Engineering and Science
Universiti Tunku Abdul Rahman**

April 2022

DECLARATION

I hereby declare that this project report is based on my original work except for citations and quotations which have been duly acknowledged. I also declare that it has not been previously and concurrently submitted for any other degree or award at UTAR or other institutions.

Signature : 

Name : Owi Chun Kit

ID No. : 1806532

Date : 22/4/2022

APPROVAL FOR SUBMISSION

I certify that this project report entitled “**STUDY OF THREE DIMENSIONAL COMPOSITE PRINTING MATERIAL THROUGH SIMULATION**” was prepared by **OWI CHUN KIT** has met the required standard for submission in partial fulfilment of the requirements for the award of Bachelor of Engineering (Honours) Mechanical Engineering at Universiti Tunku Abdul Rahman.

Approved by,

Signature	:	TJY	<hr/>
Supervisor	:	Ir. Dr. Tey Jing Yuen	<hr/>
Date	:	22/4/2022	<hr/>

The copyright of this report belongs to the author under the terms of the copyright Act 1987 as qualified by Intellectual Property Policy of Universiti Tunku Abdul Rahman. Due acknowledgement shall always be made of the use of any material contained in, or derived from, this report.

© 2022, Owi Chun Kit. All right reserved.

ACKNOWLEDGEMENTS

I would like to thank everyone who had contributed to the successful completion of this project. I would like to express my gratitude to my research supervisor, Ir. Dr. Tey Jing Yuen, for his invaluable advice, guidance and his enormous patience throughout the development of the research.

In addition, I would also like to express my gratitude to my loving parents and friends who had helped and given me encouragement throughout the completion of the entire project.

ABSTRACT

Fused Deposition Modeling (FDM) 3D printing is getting popular nowadays. It can exhibit a high degree of geometric complexity by printing with molten thermoplastic by extruding it onto a heated printing bed through a nozzle. Combining materials with different mechanical properties will be one solution to achieve a 3D printed object with functionality and desired mechanical properties. Besides, it is essential to understand how printing parameters influence the mechanical properties of a 3D printed object. This study investigates the mechanical performance of 3D composite materials with different shell and infill materials through finite element analysis. In this study, different infill patterns (triangular and hexagonal), infill density (20%, 60%, and 100%), and shell thickness (0.4 mm, 0.8 mm, and 1.2 mm) were assessed. The geometry with the stated infill pattern, infill density, and shell thickness was created using SpaceClaim software for finite element analysis. A multitools 3D printer was used to fabricate the samples and validate the experimental results obtained against finite element analysis. The tensile and flexural tests were performed according to ASTM D638 and ASTM D790. Analysis of variance was used to determine the significance level of each printing parameter. The results show that the composite PLA/PETG improved tensile strength. However, there was a decrement in flexural strength compared to PLA. Composite PLA/ABS help increase tensile and flexural strength compared to ABS. Composites PLA/PA6 had higher flexural strength compared to PA6. However, its tensile strength is lower than PLA and PA6. Composite PLA/TPU and ABS/TPU improve tensile and flexural properties compared to TPU. Composite PA6/ABS has improved tensile modulus and flexural properties, but it has lower tensile strength than PA6 and ABS. The experimental verification and validation show that the average margin of error from finite element analysis and the experimental test was lower than 10%. Through ANOVA analysis, it depicts that infill density has the lowest p-value. This indicates that infill density contributes significantly to the changes in mechanical properties. The dataset obtained from the finite element analysis can be used as a reference when fabricating 3D objects.

TABLE OF CONTENTS

DECLARATION		i
APPROVAL FOR SUBMISSION		ii
ACKNOWLEDGEMENTS		iv
ABSTRACT		v
TABLE OF CONTENTS		vi
LIST OF TABLES		viii
LIST OF FIGURES		ix
LIST OF SYMBOLS / ABBREVIATIONS		xi
LIST OF APPENDICES		xii
 CHAPTER		
1	INTRODUCTION	1
1.1	General Introduction	1
1.2	Importance of the Study	2
1.3	Problem Statement	2
1.4	Aim and Objectives	4
1.5	Scope and Limitation of the Study	4
1.6	Contribution of the Study	4
1.7	Outline of the Report	5
2	LITERATURE REVIEW	6
2.1	Introduction	6
2.2	Mechanical Properties of 3D Printed Polymer	6
2.3	Mechanical Properties of Multi-Material Composites	7
2.4	Effect of Printing Parameter on Mechanical Strength	10
2.5	Test Method	12
2.5.1	Tensile Test	12

	2.5.2 Flexural Test	13
	2.6 Summary	14
3	METHODOLOGY AND WORK PLAN	15
	3.1 Introduction	15
	3.2 Finite Element Analysis	15
	3.2.1 Create Material Model	16
	3.2.2 Create the Geometry Modelling	18
	3.2.3 Setup in ANSYS Mechanical	18
	3.3 Experimental Verification and Validation	20
	3.3.1 Materials	22
	3.3.2 Sample Fabrication	22
	3.3.3 Experimental Setup	23
4	RESULTS AND DISCUSSION	25
	4.1 Introduction	25
	4.2 Finite Element Analysis Result	25
	4.3 Effect of Printing Parameters on Mechanical Properties	28
	4.4 Experimental Verification and Validation	31
	4.4.1 Comparison of experimental and finite element analysis tensile test result	31
	4.4.2 Comparison of experimental and finite element analysis flexural test result	34
	4.5 Summary	35
5	CONCLUSIONS AND RECOMMENDATIONS	36
	5.1 Conclusions	36
	5.2 Recommendations for future work	37
	REFERENCES	38
	APPENDICES	42

LIST OF TABLES

Table 2.1: Mechanical Properties of 3D printed polymer	7
Table 2.2: Summary of the mechanical properties of multi material composites	9
Table 2.3: The mechanical properties of specimens with different infill patterns and infill density	11
Table 3.1: Variable printing parameters used for each types of materials for tensile and flexural test samples	20
Table 3.2: Fabricated multi-material tensile test specimen	20
Table 4.1: Tensile strength comparison of fabricated composite materials	33
Table 4.2 : Tensile strength comparison of fabricated composite materials	33

LIST OF FIGURES

Figure 2.1: Plot of weight for different infill patterns as function of their infill density (Ivorra-Martinez et al., 2020)	12
Figure 3.1: ANSYS simulation flow chart	15
Figure 3.2: Boundary conditions of tensile FEA	19
Figure 3.3: Boundary conditions of flexural FEA	20
Figure 3.4: Tensile test samples 3D printed with PLA (orange) and PETG (grey)	21
Figure 3.5: Flexural test samples 3D printed with PLA (orange) and PETG (grey)	21
Figure 3.6: Composites tensile test sample fabricated	21
Figure 3.7: Test setup for determining the tensile properties (left) and flexural properties (right)	24
Figure 3.8: Tensile tested specimens of PLA and PETG	24
Figure 3.9: Flexural tested specimens of PLA and PETG	24
Figure 4.1: Bubble chart of mechanical properties for each composite material and single materials obtained from FEA	26
Figure 4.2: Normalized data in percentage of mechanical properties for composites and single materials	28
Figure 4.3: Main effect of means for Tensile Strength	30
Figure 4.4: Main effect of means for Tensile Modulus	30
Figure 4.5: Main effect of means for Flexural Strength	30
Figure 4.6: Main effect of means for Flexural Modulus	30
Figure 4.7: Comparison of experimental and simulation result for tensile strength	32
Figure 4.8: Comparison of experimental and simulation result for tensile modulus	32
Figure 4.9: Samples with 0.4mm shell	33

Figure 4.10: Comparison of experimental and simulation result for flexural strength	34
Figure 4.11: Comparison of experimental and simulation result for flexural modulus	35
Figure 4.12: Bad surface finish on the top shell	35

LIST OF SYMBOLS / ABBREVIATIONS

$\sigma_{engineering}$	Engineering stress, MPa
$\varepsilon_{engineering}$	Engineering strain, mm/mm
σ_{true}	True stress, MPa
ε_{true}	True strain, mm/mm
E	Young modulus, MPa
$\varepsilon_{elastic}$	Elastic strain, mm/mm
$\varepsilon_{plastic}$	Plastic strain, mm/mm
ε_{total}	Total strain, mm/mm
C_{ij}	Cauchy strain tensor
λ_i	Stretch ratio
δ_{ij}	Extensibility parameter
I_i	Strain invariant
ABS	Acrylonitrile Butadiene Styrene
ASA	Acrylonitrile Styrene Acrylate
HIPS	High Impact Polystyrene
PA6	Polyamide 6 (Nylon 6)
PETG	Polyethylene Terephthalate Glycol
PLA	Polylactic Acid
TPU	Thermoplastic Polyurethane
3D	Three dimensional
ANOVA	Analysis of Variance
ASTM	American Society for Testing and Materials
FEA	Finite Element Analysis
FDM	Fused Deposition Modelling

LIST OF APPENDICES

Appendix A: Result from Finite Element Analysis	42
Appendix B: Comparison of Finite Element Analysis Result and Experimental Result	53

CHAPTER 1

INTRODUCTION

1.1 General Introduction

In the fourth industrial revolution, 3D printing was advantageous to humans because its production process offered various benefits over traditional manufacturing methods. The advantages include speed, flexibility, and cost-effectiveness. Every material used for 3D printing comes with different material properties, making it suitable for various applications accordingly. There are several types of 3D printing, such as Laminated Object Manufacturing (LOM), Fused Deposition Modelling (FDM), Selective Laser Melting (SLM), and Stereolithography (SLA). For desktop 3D printers, FDM is the most affordable, either for hobbyists or researchers. FDM technology creates 3D parts by layering one by one layer of melted thermoplastic filament through the extruder head of a 3D printer.

FDM technique is a popular additive manufacturing method in which parts are 3D printed layer by layer using thermoplastic materials extruded through a nozzle onto a platform. The filaments are melted and extruded onto the printing bed by the extruder. Besides, thermal fusion causes the material to bond with the layer beneath it and solidify it. FDM 3D printer can print support material to print overhang objects to achieve various goals for the final printed parts.

FDM 3D printed polymer products can exhibit a high degree of geometric complexity. Often printed products lack mechanical strength, which poses a significant barrier to their broad range of applications. Nevertheless, it is possible to solve these problems by combining different materials to achieve the desired functional and mechanical properties. As a result, there has been a lot of interest in developing composite materials for 3D printing that can be used with currently available 3D printers.

The main focus of this project is to investigate the mechanical properties of the different material composites when 3D printing with varying materials of shell and other infill materials. Besides, various shell thicknesses, infill patterns, and infill densities were used to determine the most suitable

printing parameters to get the best mechanical performance of the output product.

1.2 Importance of the Study

The importance of the project is to propose and develop a new composite for 3D printing where the material offers better strength and stiffness than 3D printing with pure thermoplastic. This study determined the effect of different material composite printing parameters on the output product to ensure it has the targeted performance characteristic. A product with different mechanical properties can be produced depending on the shell thickness, infill density, and pattern. The composite material can be used to 3D print a complex part that requires different stiffness across outer and inner layers. Since 3D printing has become very popular in the manufacturing industry, there is a need to improve the strength and durability of 3D printed products to their maximum potential. The results obtained from the project helped develop a 3D printing process and product for composite materials.

1.3 Problem Statement

3D printed parts have limited mechanical properties, and they are frequently unable to meet the mechanical requirements of functional applications. As a result of this problem, a new concept of 3D printing based on multi-material 3D printing was investigated in this study. The mechanical properties of 3D printed products can be enhanced using composite materials.

In its early stages, 3D printing with FDM technology potential was limited by the limited number of filaments available. ABS, PLA, PA6, PETG, and PC were the primary materials considered, each with its own set of applications and performance characteristics. Nowadays, users can choose filament from various options depending on the purpose of the object to be 3D printed. For example, composite thermoplastics filled with carbon or glass fibers (Goh et al., 2018), thermoplastic polyurethane (TPU), and high impact polystyrene (HIPS) (Tanikella, Wittbrodt and Pearce, 2017). However, the cost of composite thermoplastic filament is much higher compared to the regular thermoplastic filament. Few studies have been carried out to develop new composite thermoplastics for use in the FDM processes and improve the

properties of existing thermoplastics. Besides, Zhong et al., (2001) have found ways to increase the strength of ABS filament by developing short-fiber reinforced ABS composites.

The mechanical response of thermoplastic composite structures is dependent on strain rate, which affects apparent mechanical properties such as strength, stiffness, and nonlinear response. However, the effect of loading rate on the failure mode of a composite structure has been studied. Composite structure failure mechanisms and plastic deformation can be determined by failure strain localization analysis and microstructural analysis (Baranowski et al., 2019; Kucewicz et al., 2018).

Several parameters and factors affect the mechanical properties, tolerances, and overall quality of a finished product produced by the FDM process. Slicing software allows users to change many printing parameters, which affect the mechanical properties of the output product. However, there is not much information about the effect of changing the printing parameters on the mechanical performance of 3D printed parts. According to the findings of some research studies, the shell thickness, infill density, and infill pattern of a 3D printed object do impact the object's mechanical performance. 3D printed parts produced using the FDM technique have different mechanical properties affected by the printing parameters set in the slicer software (Sodeifian, Ghaseminejad and Yousefi, 2019). The fatigue response of 3D printed PLA parts using the FDM technique was investigated by Gomez-Gras et al., (2018). Other than that, Fernandez-vicente et al., (2016) determined the influence of infill patterns and infill density on the tensile behaviour of acrylonitrile-butadiene-styrene (ABS) specimens with various infill densities and infill patterns.

1.4 Aim and Objectives

The project aims to determine the mechanical performance of 3D composite material by blending two types of thermoplastics. Two objectives are outlined below:

1. To evaluate the tensile and flexural properties of 3D composite material by blending two types of thermoplastics.
2. To investigate the influence of infill pattern, infill density and shell thickness on mechanical properties of composite polymer.
3. To verify and validate the experimental results obtained against the finite element analysis results.

1.5 Scope and Limitation of the Study

The composite material used in this project was through the blending of two types of thermoplastics Polylactic Acid (PLA), Nylon 6 (PA6), Acrylonitrile Butadiene Styrene (ABS), Polyethylene Terephthalate Glycol (PETG), and Thermoplastic Polyurethane (TPU). This study covered the effect of 3D printing with several different printing parameters, such as two different infill patterns, i.e. triangular and hexagonal, three different infill densities, i.e. 20%, 60%, and 100%, and three different shell thicknesses, i.e. 0.4 mm, 0.8 mm, and 1.2 mm. This study covered two tests to determine the tensile and flexural properties according to ASTM D638 and ASTM D790 standards. The finite element analysis method was used to determine the mechanical behaviour of the composite material with different printing parameters, while few of the materials were 3D printed for experimental tests.

1.6 Contribution of the Study

This study has contributed to creating a dataset on the mechanical properties of 3D composite printing materials with various printing parameters. With the advancement of FDM 3D printing nowadays, 3D printer users want to print objects with custom properties. The investigation of this study is to determine the impact of the various printing parameters on the mechanical properties of 3D printed parts that could be helpful. This study could

contribute to an in-depth understanding of the effects of 3D printing with different materials for shell and infill.

1.7 Outline of the Report

This report consists of five chapters, including an introduction, literature review, methodology and work plan, results and discussion, and conclusions and recommendations.

Chapter 1 includes the general introduction and background of the FDM method in 3D printing. This chapter also discussed the mechanical properties of 3D printed objects, which varied against the printing parameters.

Chapter 2 reviews the mechanical properties of 3D printed polymer under tensile and flexural loading. The mechanical properties of multi-material composites 3D printed using fabricated composite filaments were revealed as the targeted mechanical performance for this study. Furthermore, the effect of the printing parameter on mechanical strength also discussed.

Chapter 3 discusses the procedures for performing the finite element analysis and experimental test. In addition, this chapter also discusses the step involved in test specimen preparation.

Chapter 4 discusses the results obtained from this project. A comparison of the result obtained for multi-material composites with single materials specimens from finite element analysis was made to observe the effect of the reinforcement. Other than that, the effect of printing parameters on mechanical properties was investigated using ANOVA analysis. In the meantime, the experimental verification and validation were discussed.

Chapter 5 concludes the finding from this project with objective accomplishment, and some recommendations were proposed for future research improvement.

CHAPTER 2

LITERATURE REVIEW

2.1 Introduction

This chapter reviews the existing research about the mechanical properties of 3D printed polymers used in the material modelling for finite element analysis in this study. This is followed by detailed information on the mechanical properties of multi-material composites as the target mechanical performance for this project. Then, the mechanical properties of the 3D printed polymer under different printing parameters were discussed. Finally, the details of the test method used in this project are outlined and investigated in this chapter.

2.2 Mechanical Properties of 3D Printed Polymer

The 3D printed PLA was found to have a tensile strength of 44.34 MPa, a tensile modulus of 1275.5MPa, and a flexural modulus of 2930 MPa (Harpool et al., 2021). Its tensile strength is 12.5% higher than PA6, 19.49% higher than ABS, 27.15% higher than PETG, and 76.32% higher than TPU.

ABS is widely used in the production of household items since it has high flexibility and low toxicity to humans. Majid et al., 2020, research show the 3D printed ABS has a tensile modulus of 1200 MPa. It is higher than PA6 (739.2 MPa), PETG (491 MPa), and TPU (14.6 MPa). However, it is 5.92 % lower than PLA.

TPU is an elastomer material for 3D printing with excellent mechanical properties and good abrasion resistance. TPU is a copolymer with soft and hard portions with a wide range of applications. In the research of Xiang et al., 2019, 3D printed TPU was found to have a high percentage of elongation at a fracture limit of 700%. Its ductility was the highest compared to PA6 (320%), PETG (8.8%), ABS (6.25%), and PLA (5.8%). However, the hardness and strength of TPU are dependent on the blend of polymers, and this is because 3D printed TPU has meager strength.

PA6 is a thermoplastic that is stronger and more brittle than TPU. In the research of Aslanzadeh et al., 2018, 3D printed PA6 was found to have a

flexural strength of 97.2 MPa. It has the highest maximum bending strength compared to PLA (84 MPa), ABS (65 MPa), PETG (44 MPa), and TPU (7.55 MPa).

PETG is a thermoplastic formed by polyethylene terephthalate (PET) and ethylene glycol. It is well known for its high impact resistance. However, 3D printed PETG was found to have a low flexural modulus of 1120 MPa (Guessasma, Belhabib and Nouri, 2019). The flexural modulus of PETG is lower than ABS (1700 MPa), PA6 (2196 MPa), and PLA (2930 MPa) but higher than TPU (156.78 MPa).

Table 2.1: Mechanical Properties of 3D printed polymer

	Tensile Strength (MPa)	Tensile Modulus (MPa)	Elongation at break (%)	Flexural Strength (MPa)	Flexural Modulus (MPa)	Citation
PA6	38.8	739.2	320	97.2	2196	Aslanzadeh et al., 2018
PLA	44.34	1275.5	5.8	84	2930	Harpool et al., 2021
ABS	35.7	1200	6.25	65	1700	Majid et al., 2020
PETG	32.3	491	8.8	44	1120	Guessasma, Belhabib and Nouri, 2019
TPU	10.5	14.6	700	7.55	156.78	Xiang et al., 2019

2.3 Mechanical Properties of Multi-Material Composites

The literature studies on the mechanical properties of the multi-material melt blended to fabricate composites filament for fabrication of samples via the FDM method are given in Table 2.2. The material properties of the multi-material composite were studied as the target mechanical performance for the composites in this project.

PLA blended with PA6 was found to have the highest tensile strength compared to the other composites. The tensile strength of the composite PLA blend with PA6 increased more than 30% when the percentage of PA6 being reinforced increased by 10%. Besides, a decrease in tensile strength was shown for composite PLA blends with TPU when the amount of TPU was increased because of the low strength of the material

TPU. Meanwhile, the composite PA6 blend with ABS was found to have a tensile strength higher than pure PA6 or ABS.

The composite PLA and ABS blend with a ratio of 7:3 was found to have the highest tensile modulus compared to other composites. Furthermore, the composite PLA blend with PETG has a tensile modulus lower than the PLA, and this is because of the low tensile modulus of PETG material blended with PLA.

In terms of the percentage of elongation at fracture, the composite PLA blended with PA6 was the highest among all the composites. The percentage of elongation at fracture of the composite decreased by 6% to 21% as the amount of PA6 reinforced increased by 10%. Other than that, a composite ABS blend with TPU helps increase elongation at break of ABS due to the flexibility of the TPU.

In summary, the composite of PLA blended with PA6 is a good material that retains the toughness of PLA while increasing the elongation at fracture when blended with PA6.

Table 2.2: Summary of the mechanical properties of multi material composites

Material		Tensile Strength (MPa)	Tensile Modulus (MPa)	Elongation at break (%)	Citation
1	PLA/PETG	28.5	1120.28	2.54	Vinyas et al., 2019
2	PLA/ABS (70%/30%)	50.9	2200	7.6	Rigoussen et al., 2019
3	PLA/PA6 (90%/10%)	65.01	-	13.95	Wu et al., 2014
4	PLA/PA6 (80%/20%)	69.45	-	10.97	
5	PLA/PA6 (70%/30%)	72.61	-	10.30	
6	PA6/ABS	55	1740	4.5	Arsad et al., 2010
7	PLA/TPU (90%/10%)	39	-	4.1	Nordin et al., 2019
8	PLA/TPU (80%/20%)	29	-	6	
9	PLA/TPU (70%/30%)	20.5	-	2.8	
10	ABS/TPU (90%/10%)	38.02	1799	8.56	Heidari et al., 2020
11	ABS/TPU (80%/20%)	34.08	1585	5.48	
12	ABS/TPU (70%/30%)	26.69	1501	7.29	

2.4 Effect of Printing Parameter on Mechanical Strength

Infill patterns, infill density, printing speed, building direction, extrusion temperatures, and layer height directly impact the mechanical strength of 3D printed parts. Alafaghani et al., (2017) proved that when infill density increases, the mechanical strength of the 3D printed part also increases. Thus, the mechanical properties of 3D printed parts increase as the weight percentage of the parts increases. Higher infill density improved the mechanical properties by providing more material to take the loads applied to the parts.

A shell is a border 3D printed by FDM for every layer. According to Sukindar et al., (2017), shell thickness has a high impact on tensile strength, and hence, to increase the mechanical strength of 3D printed parts, the shell thickness should be increased. Besides, Griffiths et al., (2016) observed that the higher weight of 3D printed objects comes from a higher number of shells. Since weight impacts the mechanical performance, the higher the weight of the 3D printed parts, the higher the mechanical strength. It was proved by the 3D printed PLA specimen with four numbers of shells having a tensile strength of 62 MPa, while the specimen with one shell had a tensile strength of 51 MPa.

Wang et al., (2020) explored the impact of infill density and infill pattern on the mechanical performance of 3D printed products by using triangular and hexagonal infill patterns and 29%, 39%, and 49% infill densities. The deterministic factor for failure modes and deformation was the infill pattern, and it is primarily a result of the errors in the printing process. However, the infill pattern has little effect on tensile strength since the result obtained by the authors shows the difference in the tensile strength is less than 10%. Meanwhile, the tensile strength increases with the increase in infill density. Table 2.3 shows the results obtained from the authors.

Table 2.3: The mechanical properties of specimens with different infill patterns and infill density

Infill pattern	Triangular			Hexagonal		
Infill density	29%	39%	49%	29%	39%	49%
Tensile strength (MPa)	2.58	3.40	4.56	2.46	3.82	4.78
Young's Modulus (MPa)	88.65	96.03	156.86	66.52	73.86	96.78

PLA 3D printed specimens with hexagonal infill patterns with 15% infill density had a 64% higher modulus of elasticity than 3D printed solid specimens (Harpool et al., 2021). It is due to the structural strength of the hexagonal infill to withstand the force applied to the specimen. Besides, the diamond infill pattern with a 15% infill density has good elastic behaviour, as its total percentage of elongation is 56% greater than that of a solid specimen. Pandzic, Hodzic and Milovanovic, (2019) proved that a concentric infill pattern with 90% infill density has the highest ultimate tensile strength and yield strength compared to other infill patterns.

Ivorra-Martinez et al., (2020) observed that the weight of the specimen is different when printed with a different infill pattern under the same infill density. The specimen 3D printed with a hexagonal infill pattern was found to have the highest weight for all infill densities. In contrast, the rectilinear and Hilbert infill patterns were ranked second and third. Since the weight of the specimen is higher, the more material it has to take the loads applied to it. Thus, the specimens with hexagonal infill have better mechanical performance than those with rectilinear or Hilbert infill patterns. However, the weight of different infill patterns is different when 3D printed with higher infill density. Due to the geometry of the infill patterns, the weight of the Hilbert infill is higher than the rectilinear infill at a density of 90%. In comparison, the weight of Hilbert infill is lower than rectilinear infill at a density of 20% (Figure 2.1). Other than that, the tensile strength of the hexagonal infill pattern increases linearly as the infill density increases because the infill pattern has excellent load distribution and excellent

cohesion. In contrast, the tensile strength of the other infill patterns does not show this effect.

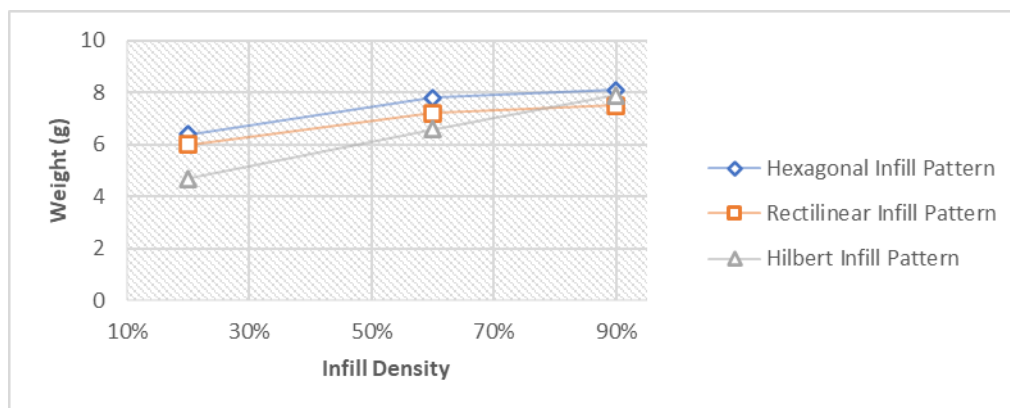


Figure 2.1: Plot of weight for different infill patterns as function of their infill density (Ivorra-Martinez et al., 2020)

2.5 Test Method

In this section, the test method used in the existing research was reviewed as the guideline for determining the mechanical response of multi-material 3D printed composites. Besides, the steps involved in performing the test through finite element analysis have also been reviewed.

2.5.1 Tensile Test

The tensile test helps determine the amount of stress present at the point of fracture (tensile strength), the maximum amount of stress exhibited by test samples (ultimate tensile strength), and the marks where plastic deformation begins (yield strength).

To characterize the ultimate tensile strength of 3D printed PETG under uniaxial loading, Özen et al., (2021) determined the material response of 3D printed parts according to ASTM D638 and ISO-527-2 standards. Meanwhile, some issues were primarily affected by prescribed curvatures, and it is difficult to fabricate using 3D printers. Rankouhi et al., (2016) performed a tensile test in accordance with the ASTM D3039 test standard to investigate the mechanical properties of an ABS specimen 3D printed by using fused deposition modelling.

ANSYS simulation software was used by Faizan and Gangwar, (2021) for finite element analysis of carbon fiber reinforced polymers. The tensile

test geometry of the composite sample is prepared in the design modeler. For the material modelling, it was imported from the ANSYS library. The first layer was defined as reinforced material, the second layer as carbon fiber, the third layer as reinforced material, the fourth layer as carbon fiber, and the fifth layer as reinforced material. One end of the specimen was set with fixed support, and the opposite end was set with the tensile force for boundary conditions.

2.5.2 Flexural Test

The flexural strength of homogeneous and isotropic material is equal to the material's tensile strength. Due to a large number of defects and strong anisotropy present in 3D printed products, flexural strength has become a difficult parameter to interpret.

Baich, Manogharan and Marie, (2015) determined the flexural strength of 3D printed ABS parts. The flexural test was performed according to the ASTM D790 standard. Durgun and Ertan, (2014) explored the effect of printing parameters on flexural strength for 3D printed ABS specimens by using a three-point bending test according to ISO 178:2006 test standard.

A three-point flexural test can be performed through ANSYS finite element analysis to investigate the flexural behaviour of polymers (Munguia, Akande and Dalgarno, 2014). The geometry of the test sample was created in CAD software with measurements of 127 mm × 12.7 mm × 3.2 mm and imported into the ANSYS workbench. The material model can be derived from experimental results obtained from lab tests. The flexural modulus obtained is used in orthotropic material definition. While for the material data such as Poisson's ratio and shear modulus, which can be obtained from the research of other researchers. A fixed constraint was applied to the flexure fixture anvil geometry. A vertical load equivalent to the experimental load range was applied to the top surface of the loading nose geometry for boundary conditions.

2.6 Summary

In a nutshell, the mechanical properties of PLA, PA6, ABS, PETG, and TPU were found to have different properties. PLA has good strength, PA6 with high ductility, PETG with high impact strength and ductility, and TPU with the highest ductility. Each material's properties were expected to help the other materials increase their mechanical performance when 3D printed with multi-materials. The mechanical properties of PLA/PETG, PLA/ABS, PLA/PA6, PA6/ABS, PLA/TPU, and ABS/TPU melt blend composites were used as the targeted performance in the finite element analysis of this study. Besides, 3D printing with a hexagonal infill pattern was found to have higher mechanical performance, and the increase in infill density and shell thickness will increase the mechanical properties. Lastly, the standards for the tensile tests of thermoplastics were there ASTM D638 standard and ASTM D790 for flexural tests.

CHAPTER 3

METHODOLOGY AND WORK PLAN

3.1 Introduction

This chapter discusses a detailed and comprehensive methodology to study the mechanical performance of 3D printed composite materials through the blending of two types of thermoplastics are discussed.

3.2 Finite Element Analysis

Figure 3.1 shows the general procedure for determining the mechanical performance of composite materials and single materials through ANSYS simulation. The finite element analysis was carried out for the materials PLA, PETG, ABS, PA6, TPU, ABS(shell)/TPU(infill), PA6(shell)/ABS(infill), PLA(shell)/ABS(infill), PLA(shell)/PA6(infill), PLA(shell)/PETG(infill), and PLA(shell)/TPU(infill). Moreover, the analysis was carried out for two infill patterns (hexagonal and triangular), three infill densities (20%, 60%, and 100%), and three shell thicknesses (0.4 mm, 0.8 mm, and 1.2 mm).

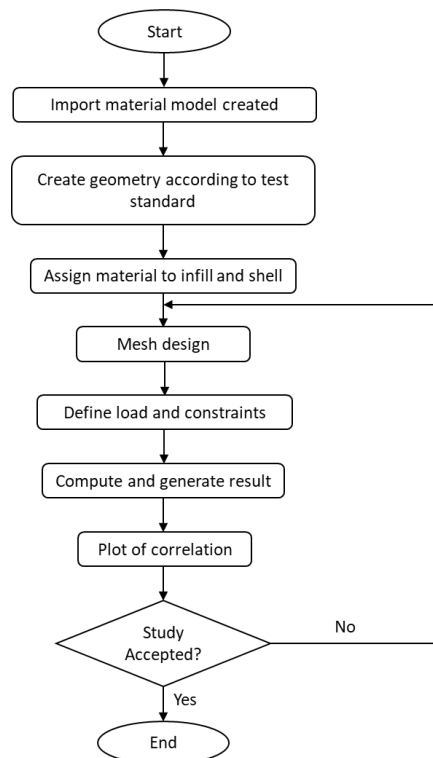


Figure 3.1: ANSYS simulation flow chart

3.2.1 Create Material Model

The engineering data of PLA, PA6, ABS, and PETG studied in the literature review was converted into true stress and strain for material modelling in ANSYS simulation using Equations 3.1 and 3.2. After getting the true stress and strain data, the elastic strain of the material can be calculated using Equation 3.3. The elastic strain calculated was used to calculate the plastic strain using Equation 3.4. At the same time, the plastic strain and true stress calculated were used in Multilinear Isotropic Hardening for the plastic deformation of the material. Besides, Young's modulus and Poisson ratio under Isotropic Elasticity was set for the elastic deformation of the material. Next, the uniaxial test data obtained from the literature review is curve fitted into the material model under uniaxial test data. Lastly, define the strength of the material by adding the tensile yield strength and ultimate tensile strength.

$$\sigma_{true} = \sigma_{engineering} \times (1 + \varepsilon_{engineering}) \quad (3.1)$$

$$\varepsilon_{true} = \ln(1 + \varepsilon_{engineering}) \quad (3.2)$$

$$\varepsilon_{elastic} = \frac{\sigma_{true}}{E} \quad (3.3)$$

$$\varepsilon_{plastic} = \varepsilon_{total} - \varepsilon_{elastic} \quad (3.4)$$

where

$\sigma_{engineering}$ = Engineering stress, MPa

$\varepsilon_{engineering}$ = Engineering strain, mm/mm

σ_{true} = True stress, MPa

ε_{true} = True strain, mm/mm

E = Young's modulus, MPa

$\varepsilon_{elastic}$ = Elastic strain

$\varepsilon_{plastic}$ = Plastic strain

ε_{total} = Total strain

For TPU, uniaxial test data obtained from the literature review was used to curve fit the hyperelastic material model in engineering data using the Mooney-Rivlin five Parameters. A five parameter Mooney-Rivlin model (Polymerdatabase, 2020) was chosen to obtain more accurate results for TPU. Equation 3.5 shows the equation of strain energy density, which can be used to derive the stress-strain relationships of TPU.

$$w = C_{10}(I_1 - 3) + C_{01}(I_2 - 3) + C_{20}(I_1 - 1)^2 + C_{02}(I_2 - 3)^2 + C_{11}(I_1 - 3)(I_2 - 3) \quad (3.5)$$

The Cauchy strain tensor C includes the reciprocal extension or stretch ratios, defined as the deformations of a cubic volume element along the principal axes.

$$C_{ij} = \delta_{ij}\lambda_i^{-2} \quad (3.6)$$

$$\lambda_i = 1 + \varepsilon_{engineering} \quad (3.7)$$

The two strain invariants are used to define the strain energy density function.

$$I_1 = \lambda_1^2 + \lambda_2^2 + \lambda_3^2 \quad (3.8)$$

$$I_2 = \lambda_1^2\lambda_2^2 + \lambda_2^2\lambda_3^2 + \lambda_3^2\lambda_1^2 \quad (3.9)$$

where

C_{ij} = Cauchy strain tensor

λ_i = Stretch ratio

δ_{ij} = Extensibility parameter

I_i = Strain invariant

3.2.2 Create the Geometry Modelling

SpaceClaim in ANSYS was used to create the geometry with different infill densities, infill patterns, and shell thicknesses using the shell function. The specimen dimensions were created according to ASTM D638–Type IV for tensile test specimens and the ASTM D790 standard for flexural test specimens. The tensile test specimen was created without the radius of the fillet to be able to split the body of the shell and infill of the specimens. In Figure 3.2, a tensile test specimen with a hexagonal 20% infill and a shell thickness of 0.4 mm was shown. Besides, flexural test specimens were shown in Figure 3.3, with two support spans and a load cell included in the geometry modelled for flexural tests.

3.2.3 Setup in ANSYS Mechanical

For tensile finite element analysis, the geometry of the shell was selected in the model tree and assigned its material. The same step was repeated by adding the infill material. Next, the mesh was created for the shell and infill. Grid independent tests were carried out in choosing the element size and method to ensure the accuracy of the simulated results. For the shell, body sizing with an element size of 2 mm was defined, while an element size of 1 mm and a patch conforming method were defined for the infill. A name selection was created for the area of interest on the tensile specimen. The body of infill and shell at the area of interest was selected and right-clicked to choose a name, defining it as the area of interest. Besides, the boundary conditions and analysis settings were set under the static structural tab. Large deflection and auto time stepping are turned on, and initial substeps are set to 30, with a minimum substep of 30 and a maximum substep of 1000 for the analysis setting. For boundary conditions, fixed support was set at one end of the specimens, and a displacement of 50 mm was set on the other end, as shown in Figure 3.2. Displacement was set to simulate a pulling rate of 5 mm/min according to the ASTM D638 standard. In the solution section, equivalent stress and equivalent total strain on the area of interest were created.

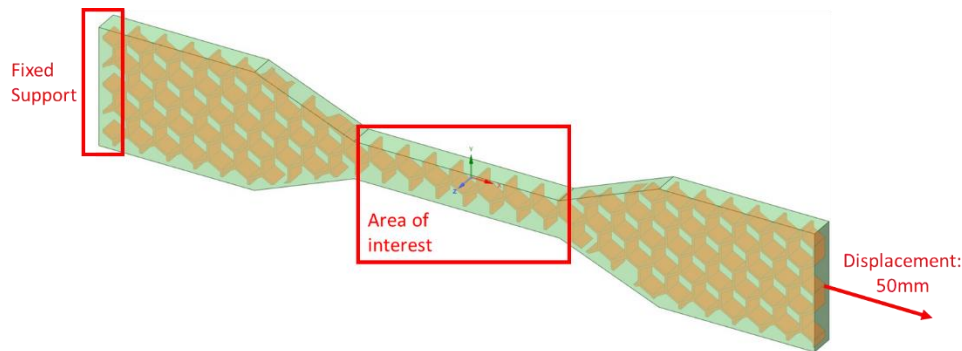


Figure 3.2: Boundary conditions of tensile FEA

For flexural finite element analysis, the steps in assigning material to the shell and infill were the same as tensile FEA. However, the support spans and load cell were assigned as a structural steel in flexural FEA. Proceed with defining the contact status between the load cell and support spans with the test specimen. Rough contact was set between the load cell and the test specimen, while frictional contact was set between the support spans and the test specimen. While the contact between shell and infill was set as bonded. Next, a joint connection was created to define the bottom part of the support spans as fixed to the ground and a translational joint on the load cell. For mesh, grid-independent tests were carried out in choosing the element size and method to ensure the accuracy of the simulated results. The specimen shell was set with an element size of 2 mm. The infill was defined with an element size of 1 mm and a patch conforming method. Aside from that, the created translational joint is dragged to the static structural to define the boundary condition of 50 mm displacement in the X direction (Figure 3.3). Displacement was set to simulate a pushing of 2 mm/min according to ASTM D790 standard. Meanwhile, the large deflection was turned on in the analysis setting, and auto time stepping was turned on. Initial substeps were set to 20, with a minimum substep of 20 and a maximum of 100. Lastly, equivalent stress and equivalent total strain of the shell and infill bodies of the specimen were created.

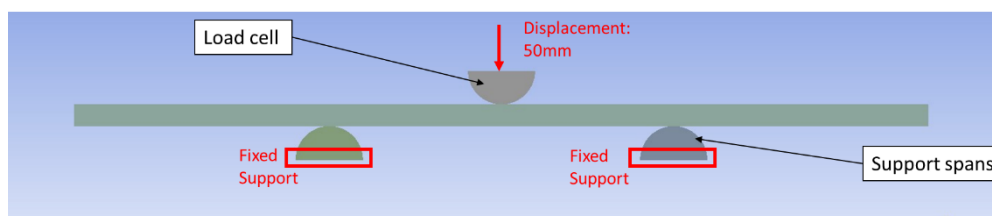


Figure 3.3: Boudary conditions of flexural FEA

3.3 Experimental Verification and Validation

Tensile and flexural test samples were 3D printed according to ASTM D638 and ASTM D790 standards to validate the experimental results obtained against the simulation results. The experimental tests were carried out for two infill patterns, three infill densities, and two shell thicknesses for PLA and PETG, as shown in Table 3.1.

Three samples of multi-material tensile test specimens were fabricated for experimental testing (Figure 3.6). The printing parameters and material of the composite are shown in Table 3.2.

Table 3.1: Variable printing parameters used for each types of materials for tensile and flexural test samples

Infill pattern	Infill density (%)	Shell thickness (mm)	Total sample
Hexagonal	20	0.4	3
	60	0.4	3
	20	0.8	3
	60	0.8	3
Triangular	20	0.4	3
	60	0.4	3
	20	0.8	3
	60	0.8	3
	100	0.8	3

Table 3.2: Fabricated multi-material tensile test specimen

Material	Infill pattern	Infill density (%)	Shell thickness (mm)
PLA/PETG	Rectilinear	100	1.2
Shell: PLA Infill: PETG	Triangular	60	1.2
PLA/TPU	Rectilinear	100	0.8
Shell: PLA Infill: TPU			



Figure 3.4: Tensile test samples 3D printed with PLA (orange) and PETG (grey)

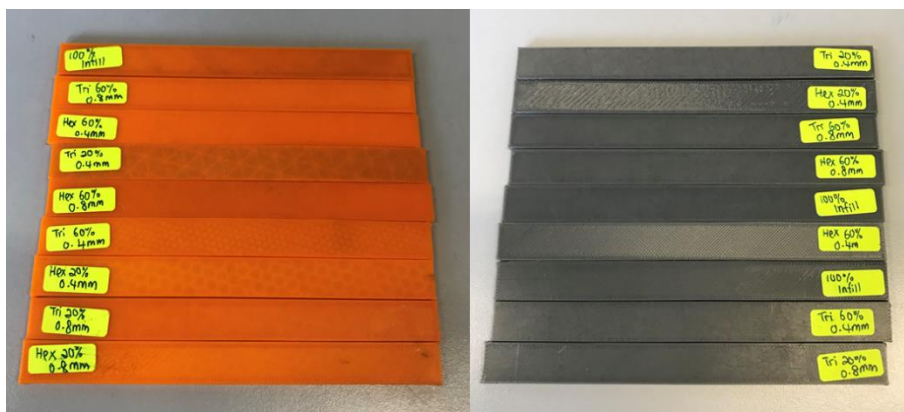


Figure 3.5: Flexural test samples 3D printed with PLA (orange) and PETG (grey)



Figure 3.6: Composites tensile test sample fabricated

3.3.1 Materials

This experimental test used three commercially available 3D printing filaments, TPU, PLA, and PETG 1.75mm filaments supplied by SUNLU. The PLA filament comes with a recommended printing temperature of 210 °C to 235 °C and a recommended bed temperature of 60 °C to 80 °C. While the PETG' s recommended printing temperature was 230 °C to 250 °C, and the recommended bed temperature was 80 °C to 120 °C. Moreover, TPU' s recommended printing temperature was 205 °C to 230 °C, and it was recommended to print without bed heating. The filaments were shipped and kept in a sealed box with a silica gel desiccant packet to prevent moisture absorption by the material. Besides, each spool of the filament comes in a vacuum-sealed condition.

3.3.2 Sample Fabrication

The test sample was fabricated by using a multitoools 3D printer. PrusaSlicer software set all the printing parameters and generated the g-code for 3D printing.

In PrusaSlicer 2.4.1, layers and perimeters under print settings were set according to the shell thickness mentioned. To print a 0.4 mm shell thickness, one perimeter with two horizontal shells on top and bottom was set in the print setting. Two perimeters with four horizontal shells were set to 3D print a 0.8 mm shell thickness, and three perimeters with six horizontal shells were set to 3D print 1.2 mm shell thickness. Fill density and the fill pattern were set under the print setting tab for infill.

Meanwhile, for each variable printing parameter set, three samples for each specimen were fabricated for testing to guarantee the repeatability of the test results. The other printing parameters not included in the study area have been kept constant during all the 3D printing processes. The constant printing parameters used in fabricating the test sample are shown in Table 3.3.

Table 3.3: Constant printing parameters used in 3D printing the test sample

Layer height	0.2mm
Raster angle	45°
Nozzle diameter	0.4mm
Filament diameter	1.75mm
Printing temperature for PLA	220 °C
Bed temperature for PLA	60 °C
Printing temperature for PETG	230 °C
Bed temperature for PETG	80 °C
Printing temperature for TPU	230 °C

3.3.3 Experimental Setup

For tensile and flexural experimental tests, a Shimadzu servo-hydraulic dynamic universal testing machine (EHF-EM050K1-020-0A) was used (Figure 3.7). For the tensile test, hydraulic grips were installed on the upper and bottom parts of the testing machine. The displacement rate of 5 mm/min and the dimension of the test sample was set in the Shimadzu Gluon software. After setup, the tests were carried out on all 3D printed tensile test specimens. Figure 3.8 shows the specimens of PLA and PETG after being tested under tensile loading.

Besides, Shimadzu servo-hydraulic dynamic universal testing machine jigs changed to the three-point bending flexural test load cell and support spans. The distance between support spans was according to the ASTM D790 standard, which is 16 times the depth of the specimen, 51.2 mm. The load cell was set close to the test specimen before starting the test. The loading rate was set to 2 mm/min, and the dimension of the specimen was input into the Shimadzu Gluon software. Figure 3.9 shows the specimens of PLA and PETG after being tested under flexural loading.



Figure 3.7: Test setup for determining the tensile properties (left) and flexural properties (right)



Figure 3.8: Tensile tested specimens of PLA and PETG

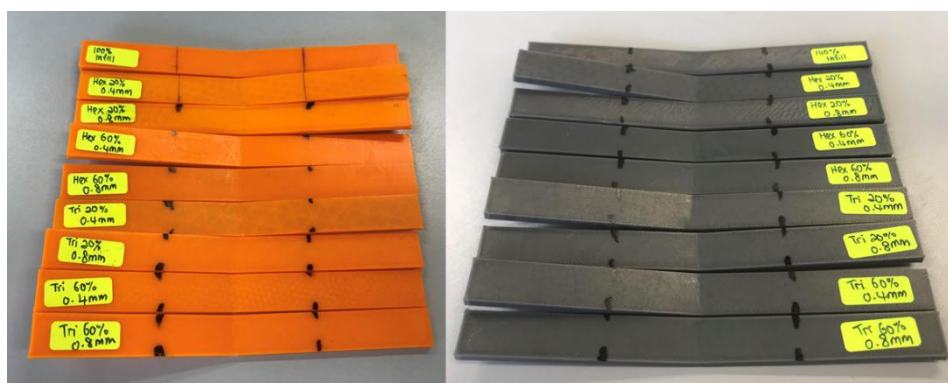


Figure 3.9: Flexural tested specimens of PLA and PETG

CHAPTER 4

RESULTS AND DISCUSSION

4.1 Introduction

This chapter investigates the mechanical properties of 3D printed composite materials through the discrete blending of two types of thermoplastics in simulation. The effect of blending each of the materials has been discussed. Besides, the results obtained through analysis of variance were used to examine each printing parameter's influence on the composites' mechanical properties. The results obtained from the experimental tensile and flexural tests for PLA and PETG were compared with the finite element analysis to discuss the margin error.

4.2 Finite Element Analysis Result

The finite element analysis result is obtained and shown in Appendix A. Besides, a bubble chart (Figure 4.1) was used to depict and show the relationships between tensile strength, tensile modulus, and flexural strength of the specimen with 100% infill density and 0.8 mm shell for each composite material and the single material. The size of the bubbles indicates the flexural strength of each material.

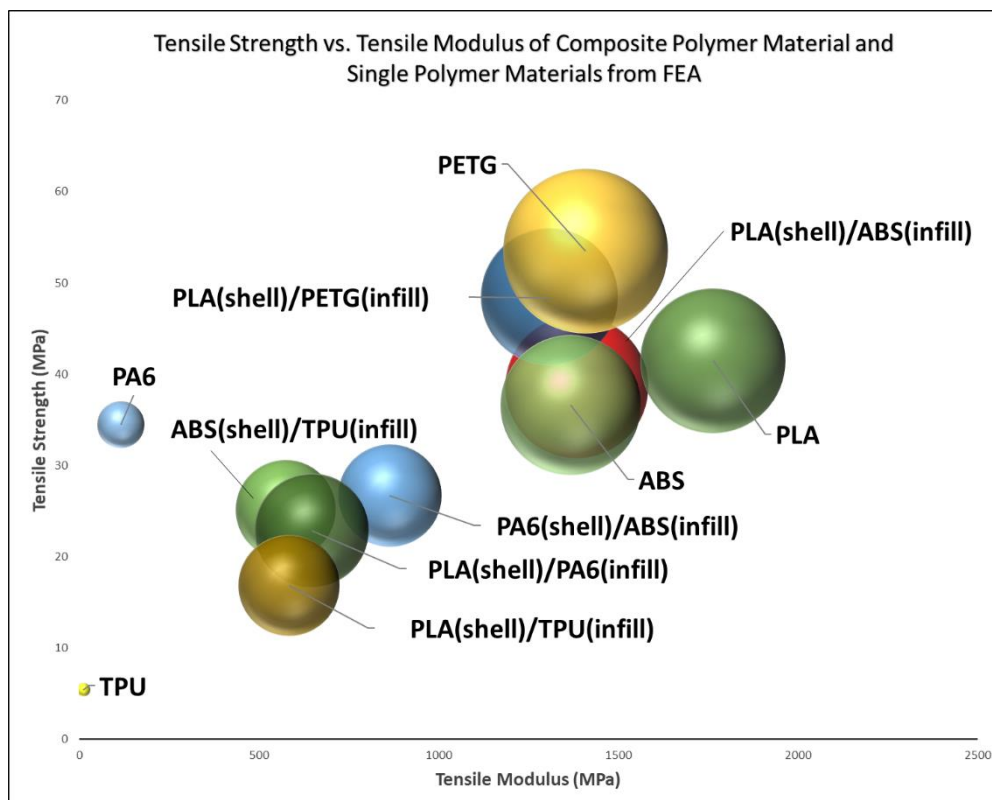


Figure 4.1: Bubble chart of mechanical properties for each composite material and single materials obtained from FEA

Figure 4.2 shows normalized data in percentages of each composite compared with single materials.

For the composite ABS/TPU (ABS shell and TPU infill), the ABS shell increased the mechanical properties of the composite compared to TPU. The ABS shell increases the toughness of TPU by more than three times the tensile strength of TPU. The strength of the composites mainly comes from the strength of the ABS shell. These results were shown the same as the observation from Heidari et al., (2020) study, which stated the ABS blend with TPU showed an increment of tensile strength. Meanwhile, the flexural strength of composite ABS/TPU and TPU has a difference of 98.17%. Lastly, the stiffness of the composite is lower than ABS but much higher than TPU.

The composite PA6/ABS (PA6 shell and ABS infill) was targeted to have high flexibility and stiffness compared to PA6. The composite PA6/ABS has lower tensile strength than PA6 and ABS. Meanwhile, the research carried out by Arsad et al., (2010) proved that a composite PA6 blend with ABS has a tensile strength higher than PA6 and ABS. This difference finding was due to the ratio of PA6 and ABS blend by the authors

is 60:40, which has higher PA6 content, while the ratio of volume for PA6 shell and ABS infill for specimen with 0.8mm shell with 100% infill is 48:52, and which has higher ABS content. However, the composite PA6/ABS has higher flexibility and stiffness than PA6, and the result comes from the flexural strength and flexural modulus of the ABS infill.

The tensile strength of PLA/ABS composites (PLA shell and ABS infill) is lower than PLA but higher than ABS. This result indicates that the toughness of PLA helps in increasing the tensile strength of ABS by 5.15% with the PLA shell. Besides, PLA/ABS composites has a tensile modulus nearly the same as ABS, although PLA has a higher tensile modulus. It might be due to the volume percentage of PLA in the composites being too low. The finding has matched the result of Rigoussen et al., (2019), which has found that the composite PLA and ABS blend has the highest tensile modulus compared to other composites. Besides, the flexural strength of PLA/ABS is higher than that of ABS but lower than PLA by 2.755%. Meanwhile, the difference between the flexural modulus of the PLA/ABS and PLA was only 3.5%.

The result shows that PLA/PETG (PLA shell and PETG infill) has tensile strength 14.47% higher than PLA. However, the tensile modulus of PLA/PETG was lower compared to PLA since the tensile modulus of PLA is 20.1% higher than PETG. It is because PLA 0.8mm shell volume occupied only 8.45% of the whole volume of the samples; more than 90% of the material is the PETG infill. PLA/PETG was found to have less strength and stiffness than PLA and PETG. The finding shows the same result from Vinyas et al., (2019) study, where the composites PLA/PETG has lower flexural modulus than PLA. It was mainly due to the properties of PETG, which was brittle.

The mechanical properties change when the discrete blend of PLA/TPU (PLA shell and TPU infill) shows the same response as the composite ABS/TPU. The result indicates that TPU has the lowest result in tensile strength, tensile modulus, flexural strength, and flexural modulus. However, the composite PLA/TPU with a 0.8 mm PLA shell was able to increase the tensile strength by two times the toughness of the TPU, increase the tensile modulus by 56 times the flexibility of the TPU, increase the

flexural strength by 5337%, and increase the flexural modulus by almost 10000%. The better mechanical properties are mainly from the PLA blended with TPU in this study.

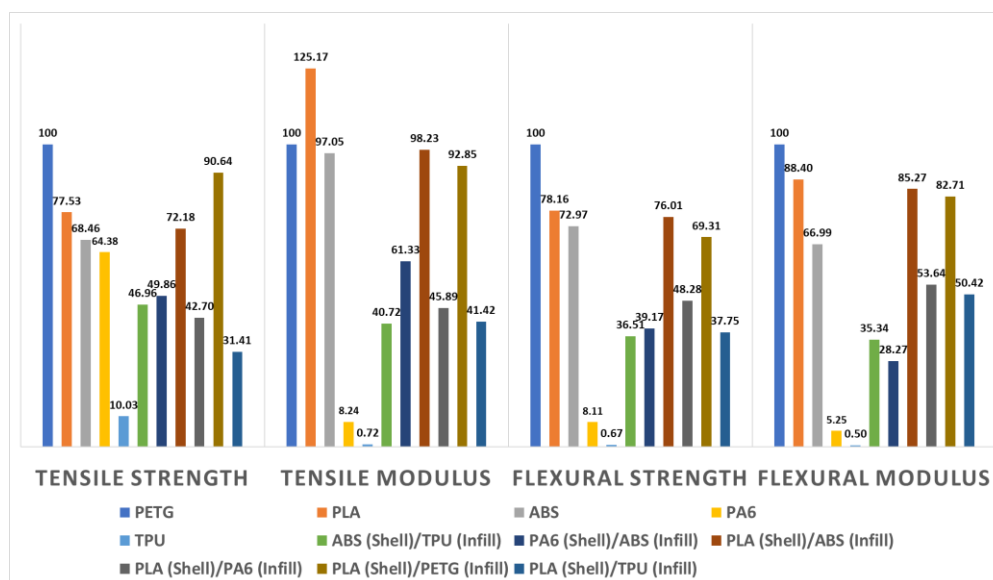


Figure 4.2: Normalized data in percentage of mechanical properties for composites and single materials

4.3 Effect of Printing Parameters on Mechanical Properties

An ANOVA analysis was performed on the dataset obtained to determine which printing parameters have the most significant effect on the mechanical properties of composite materials. The analysis was performed for each of the mechanical properties of the specimen, tensile strength, tensile modulus, flexural strength, and flexural modulus. The p-values obtained from the ANOVA analysis were compared with a significance level of 5% to validate the statistical significance of the variable printing parameters included in the finite element analysis.

For tensile strength, the most significant printing parameter was infill density. The line graph is shown in Figure 4.3 shreds of evidence that the infill density directly correlates with the tensile strength since it has the lowest p-value. It can be related to the sample having more materials to take the load when infill density is higher. Meanwhile, the ANOVA analysis result showed that the p-value of shell thickness is not much higher than 0.05,

indicating that shell thickness can be considered the printing parameter that affects the tensile strength. Nevertheless, the infill pattern does not significantly affect tensile strength. The highest tensile strength can be obtained from a triangular 100% infill sample and a 1.2 mm shell.

Obtained p-values for tensile modulus indicate infill density has the most significant influence, as shown in Figure 4.4. At the same time, the shell thickness can also be considered a printing parameter that affects the tensile modulus. The sample with the highest tensile modulus can be obtained from a sample with a hexagonal 100% infill and a 1.2 mm shell.

In the case of flexural strength, the printing parameters shell thickness and infill pattern have less influence on flexural strength than infill density, which has a remarkable effect on the flexural strength as it has very low p-values, as shown in Figure 4.5. ANOVA analysis showed that the highest flexural strength was obtained from the sample with 100% infill density, hexagonal infill pattern, and 0.4mm shell thickness.

Figure 4.6 indicates that infill density has the most significant effect on flexural modulus. The ANOVA result showed that to get samples with high flexural modulus, the printing parameter of infill density was the only parameter that has to be taken into account. This was due to the infill density having the most significant effect on the amount of the material of the samples to withstand the flexural load applied to the specimens. In contrast, shell thickness and infill pattern do not influence the flexural modulus. However, samples with 60% infill density have lower flexural modulus than samples with 20% infill density.

From the result, infill density was the printing parameter that affected the mechanical properties the most. It was mainly due to the result from the finite element analysis showing the tensile and flexural properties increased when the infill density increased. Besides, due to the thickness of the samples for both tensile and flexural tests according to ASTM D638 and ASTM D790 having a thin thickness, in the meantime, this study couldn't cover samples with higher shell thickness. In contrast, the difference of each shell thickness studied was 0.2mm, causing the effect of changing shell thickness to be lower.

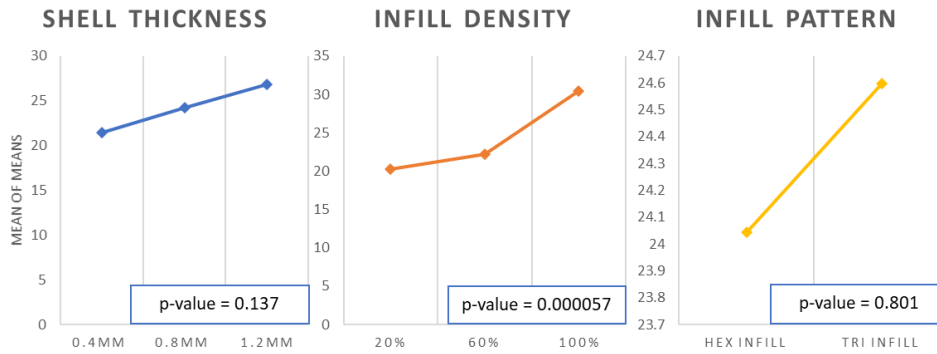


Figure 4.3: Main effect of means for Tensile Strength

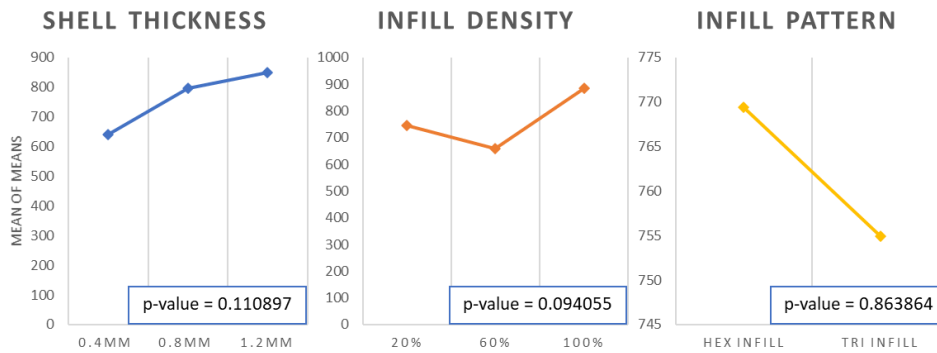


Figure 4.4: Main effect of means for Tensile Modulus

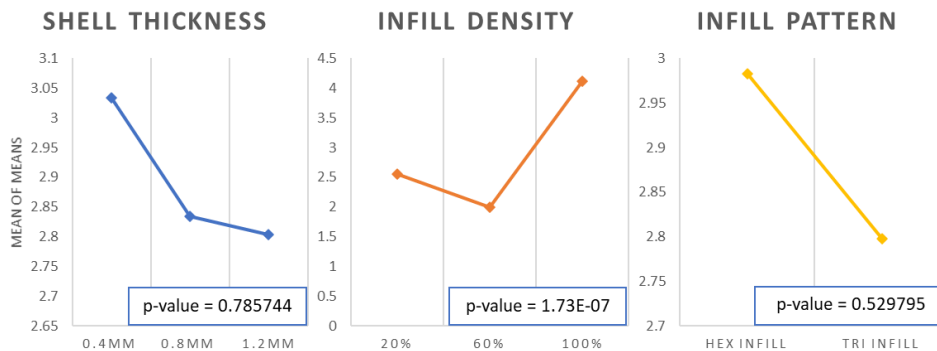


Figure 4.5: Main effect of means for Flexural Strength

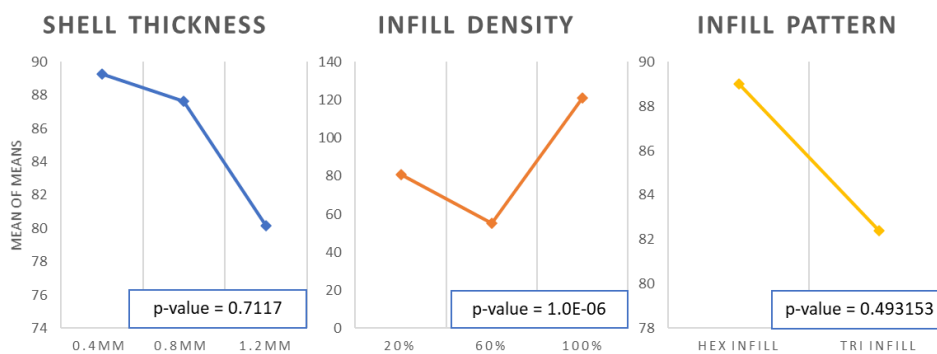


Figure 4.6: Main effect of means for Flexural Modulus

4.4 Experimental Verification and Validation

The experimental tensile and flexural test was conducted to verify and validate the experimental result against the simulation results. The experimental and simulation results in comparison were shown in Appendix B with the error margin percentage. A series of results from experimental and simulation of specimens with various printing parameters were used to create a box plot to illustrate the difference between experimental and simulation results.

4.4.1 Comparison of experimental and finite element analysis tensile test result

The bar chart in Figures 4.7 and 4.8 shows the comparison of experimental and simulation results for the tensile properties of PLA and PETG. The red line in the bar chart indicates the error margin of experimental and simulation results. The average error margin is below 10%. However, several results have an error margin higher than 30%. The high error margin mostly comes from the result of the specimen with 0.4 mm shell thickness. This is because the shell thickness is too thin, which causes the samples to dent (Figure 4.9) when clamped with the jigs during the experimental tensile test, which caused the experimental result to be much lower than the simulation result. This might also happen because the specimen's shape in finite element analysis was created without the fillet radius, while the experimental specimen comes with the radius of the fillet. The finite element analysis result was higher than the experimental result due to the higher stress concentration on the specimen without the fillet radius in finite element analysis.

In addition, Tables 4.1 and 4.2 compare experimental and simulation results for the composites PLA/PETG and PLA/TPU. The difference between experimental and simulation results for PLA/TPU composites was higher than 30%. This is due to the mechanical properties of TPU (Xiang et al., 2019) obtained from a literature review used to create material models for FEA that was slightly different from the TPU used to fabricate the composite sample. Besides, the adhesion between the infill and shell was set as bonded in finite element analysis. However, insufficient adhesion between PLA and TPU was

found when 3D printing TPU material on PLA using FDM method (Brancewicz-Steinmetz, Sawicki and Byczkowska, 2021).

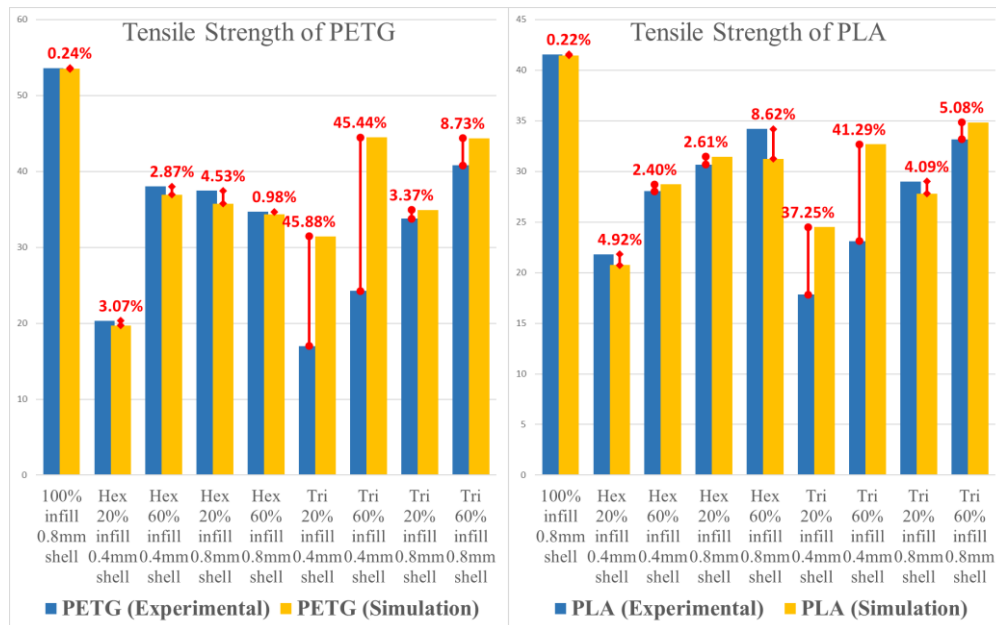


Figure 4.7: Comparison of experimental and simulation result for tensile strength

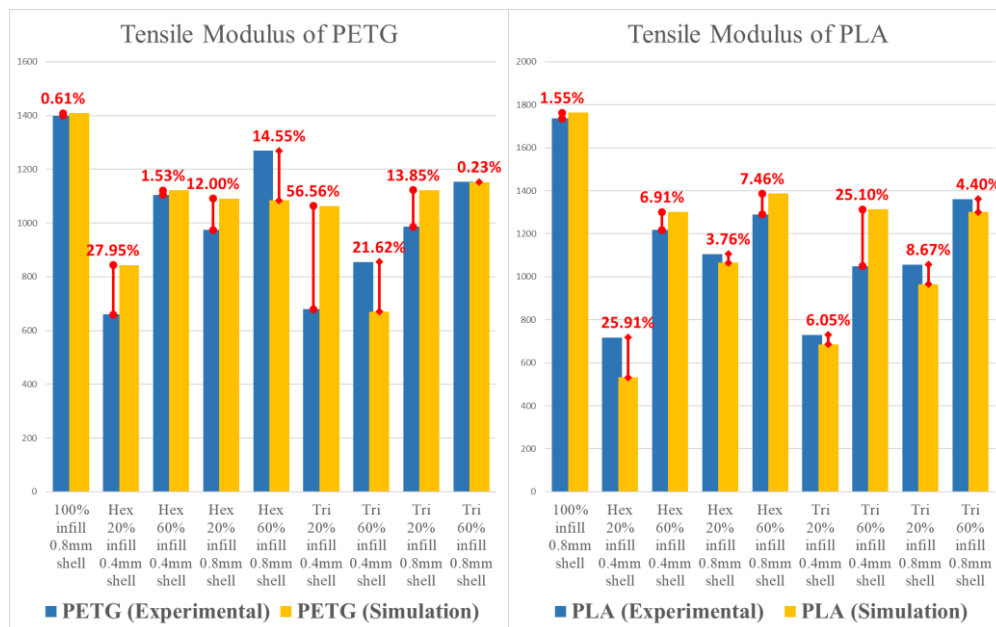


Figure 4.8: Comparison of experimental and simulation result for tensile modulus

Table 4.1: Tensile strength comparison of fabricated composite materials

	Experimental Result (MPa)	Simulation Result (MPa)	Error margin (%)
PLA/PETG			
100% Infill 0.8mm shell	49.9891	46.962	6.0555
Tri 60% Infill 0.8mm shell	37.5222	34.151	8.9848
PLA/TPU			
100% Infill 1.2mm shell	24.991	16.798	32.7833

Table 4.2 : Tensile strength comparison of fabricated composite materials

	Experimental Result (MPa)	Simulation Result (MPa)	Error margin (%)
PLA/PETG			
100% Infill 0.8mm shell	1518.6	1344.8	11.4448
Tri 60% Infill 0.8mm shell	1382.5	1206.4	12.7378
PLA/TPU			
100% Infill 1.2mm shell	992.3	583.38	41.2093



Figure 4.9: Samples with 0.4mm shell

4.4.2 Comparison of experimental and finite element analysis flexural test result

The bar chart in Figures 4.10 and 4.11 compares experimental and simulation results for the flexural properties of PLA and PETG. The red line in the bar chart indicates the error margin of experimental and simulation results. The average error margin is lower than 10%. Meanwhile, PETG samples of triangular 20% infill with a 0.4 mm shell have an error margin of 19.44%. This is because the top shell of the fabricated samples was of poor quality, as shown in Figure 4.12. This occurred due to the lower infill density with thin shell thickness, which caused the under extrusion. This problem can be solved by reducing the bridging speed and increasing the bridge flow rate in the print setting. Hence, it can be concluded that the experimental result validated the finite element analysis result since the average error margin is low.

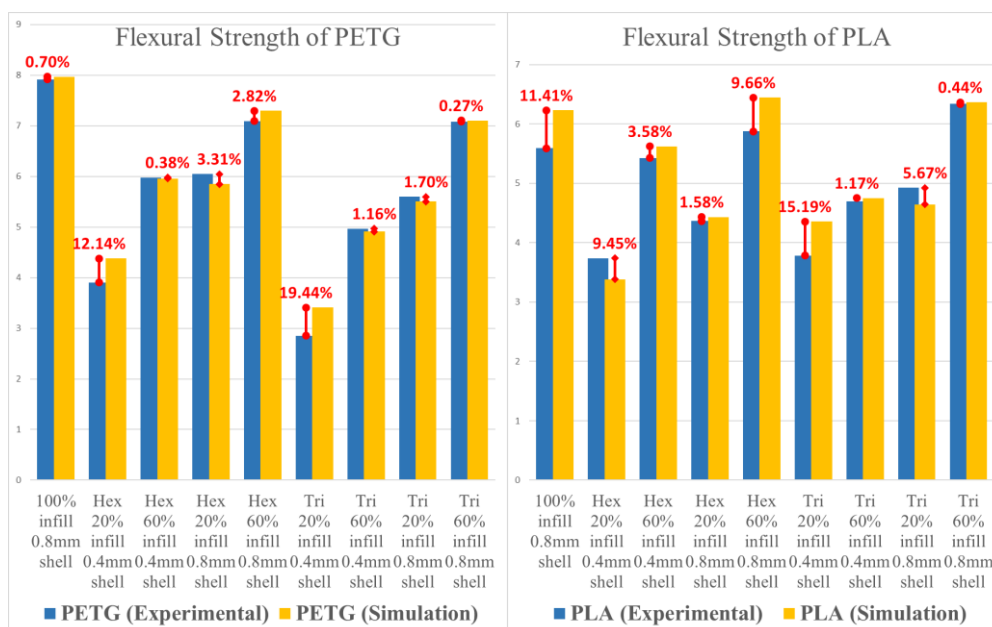


Figure 4.10: Comparison of experimental and simulation result for flexural strength

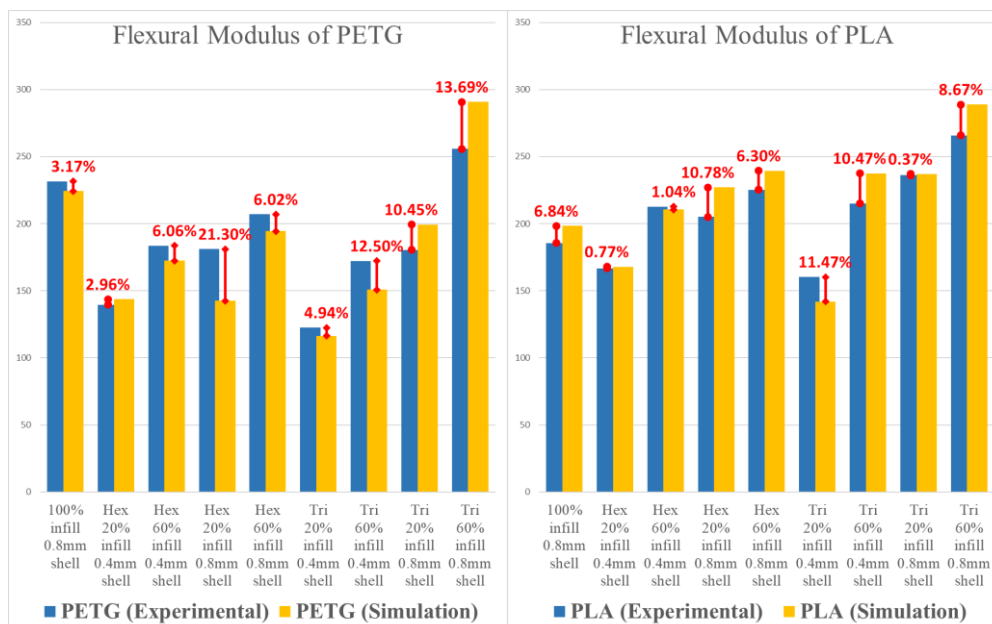


Figure 4.11: Comparison of experimental and simulation result for flexural modulus



Figure 4.12: Bad surface finish on the top shell

4.5 Summary

The finite element analysis result has proven changes in tensile strength, tensile modulus, flexural strength, and flexural modulus when discrete blending two types of thermoplastic material in print. Besides, the result of ANOVA analysis proved that infill density influences the mechanical properties of a 3D printed object the most. The results from the experiment have shown that results from the finite element analysis match up with the results from the experiment.

CHAPTER 5

CONCLUSIONS AND RECOMMENDATIONS

5.1 Conclusions

The mechanical performance of multi-material composite print objects was obtained through finite element analysis performed using ANSYS software. The result of FEA shows the composites PLA/PETG had an improvement in tensile strength but a decrease in flexural strength compared to PLA. Composite PLA/ABS helped in increasing tensile and flexural strength. Compared to ABS, composite PLA/PA6 had higher flexural strength when compared to PA6. However, with a decrement in tensile strength compared to PLA and PA6, composite PA6/ABS improved tensile modulus and flexural properties. However, it has lower tensile strength than PA6 and ABS and composites PLA/TPU, and ABS/TPU were improved tensile and flexural properties compared to TPU.

Besides, the results obtained from the experimental tensile and flexural tests have verified the results obtained from the finite element analysis, which indicates higher confidence levels in the obtained result since the average error margin is low. The finite element analysis results obtained using ANSYS software can effectively predict the mechanical performance of the samples under tensile loading and flexural loading.

Lastly, ANOVA analysis results helped investigate the impact of each printing parameter that affects the mechanical properties of the composite print object. The printing parameter that has the most significant effect on the mechanical properties is infill density.

5.2 Recommendations for future work

The study of 3D composite printing materials through simulation is still in its infancy stage. There is potential for a more in-depth investigation to determine which material combination can provide better mechanical performance. It is recommended to perform more analysis on the material TPU, as it comes with unique mechanical properties. Investigation of composite with TPU shell might bring more desired outcomes. Since TPU is a flexible material, it can act as a flexible coating on another material to help the material take the impact load applied to it. Impact testing should be done to investigate the structural flexibility of the composite.

REFERENCES

- Alafaghani, A., Qattawi, A., Alrawi, B. and Guzman, A., 2017. Experimental Optimization of Fused Deposition Modelling Processing Parameters: A Design-for-Manufacturing Approach. *Procedia Manufacturing*, [online] 10, pp.791–803. Available at: <<http://dx.doi.org/10.1016/j.promfg.2017.07.079>>.
- Arsad, A., Rahmat, A.R., Hassan, A. and Iskandar, S.N., 2010. Mechanical and rheological properties of PA6/ABS blends - With and without short glass fiber. *Journal of Reinforced Plastics and Composites*, 29(18), pp.2808–2820.
- Aslanzadeh, S., Saghlatoon, H., Honari, M.M., Mirzavand, R., Montemagno, C. and Mousavi, P., 2018. Investigation on electrical and mechanical properties of 3D printed nylon 6 for RF/microwave electronics applications. *Additive Manufacturing*, [online] 21(December 2017), pp.69–75. Available at: <<https://doi.org/10.1016/j.addma.2018.02.016>>.
- Baich, L., Manogharan, G. and Marie, H., 2015. Study of infill print design on production cost-time of 3D printed ABS parts. *International Journal of Rapid Manufacturing*, 5(3/4), p.308.
- Baranowski, P., Płatek, P., Antolak-Dudka, A., Sarzyński, M., Kucewicz, M., Durejko, T., Małachowski, J., Janiszewski, J. and Czujko, T., 2019. Deformation of honeycomb cellular structures manufactured with Laser Engineered Net Shaping (LENS) technology under quasi-static loading: Experimental testing and simulation. *Additive Manufacturing*, [online] 25(November 2018), pp.307–316. Available at: <<https://doi.org/10.1016/j.addma.2018.11.018>>.
- Brancewicz-Steinmetz, E., Sawicki, J. and Byczkowska, P., 2021. The influence of 3d printing parameters on adhesion between polylactic acid (PLA) and thermoplastic polyurethane (tpu). *Materials*, 14(21).
- Durgun, I. and Ertan, R., 2014. Experimental investigation of FDM process for improvement of mechanical properties and production cost. *Rapid Prototyping Journal*, 20(3), pp.228–235.
- Faizan, M. and Gangwar, S., 2021. Tensile behaviour of carbon fiber reinforced polymer composite using ANSYS 21. *Materials Today: Proceedings*, [online] (xxxx). Available at: <<https://doi.org/10.1016/j.matpr.2021.03.724>>.
- Fernandez-vicente, M., Calle, W., Ferrándiz, S. and Conejero, A., 2016. Effect of Infill Parameters on Tensile Mechanical Behavior in Desktop 3D Printing. *3D Printing and Additive Manufacturing*, 3, pp.183–192.

Goh, G.D., Dikshit, V., Nagalingam, A.P., Goh, G.L., Agarwala, S., Sing, S.L., Wei, J. and Yeong, W.Y., 2018. Characterization of mechanical properties and fracture mode of additively manufactured carbon fiber and glass fiber reinforced thermoplastics. *Materials and Design*, [online] 137, pp.79–89. Available at: <<https://doi.org/10.1016/j.matdes.2017.10.021>>.

Gomez-Gras, G., Jerez-Mesa, R., Travieso-Rodriguez, J.A. and Lluma-Fuentes, J., 2018. Fatigue performance of fused filament fabrication PLA specimens. *Materials and Design*, [online] 140, pp.278–285. Available at: <<https://doi.org/10.1016/j.matdes.2017.11.072>>.

Griffiths, C.A., Howarth, J., Rowbotham, G.D.A. and Rees, A., 2016. Effect of Build Parameters on Processing Efficiency and Material Performance in Fused Deposition Modelling. *Procedia CIRP*, [online] 49, pp.28–32. Available at: <<http://dx.doi.org/10.1016/j.procir.2015.07.024>>.

Guessasma, S., Belhabib, S. and Nouri, H., 2019. Printability and tensile performance of 3D printed polyethylene terephthalate glycol using fused deposition modelling. *Polymers*, 11(7).

Harpool, T.D., Alarifi, I.M., Alshammari, B.A., Aabid, A., Baig, M., Malik, R.A., Sayed, A.M., Asmatulu, R. and El-Bagory, T.M.A.A., 2021. Evaluation of the infill design on the tensile response of 3d printed polylactic acid polymer. *Materials*, 14(9), pp.1–21.

Heidari, F., Aghalari, M., Chalabi Tehran, A. and Shelesh-Nezhad, K., 2020. Study on the fluidity, mechanical and fracture behavior of ABS/TPU/CNT nanocomposites. *Journal of Thermoplastic Composite Materials*.

Ivorra-Martinez, J., Quiles-Carrillo, L., Lascano, D., Ferrandiz, S. and Boronat, T., 2020. Effect of infill parameters on mechanical properties in additive manufacturing. *Dyna (Spain)*, 95(4), pp.412–417.

Kucewicz, M., Baranowski, P., Małachowski, J., Popławski, A. and Płatek, P., 2018. Modelling, and characterization of 3D printed cellular structures. *Materials and Design*, 142, pp.177–189.

Majid, F., Zekeriti, N., Rhanim, R., Lahlou, M., Rhanim, H. and Mrani, B., 2020. Mechanical behavior and crack propagation of ABS 3D printed specimens. *Procedia Structural Integrity*, [online] 28(2019), pp.1719–1726. Available at: <<https://doi.org/10.1016/j.prostr.2020.10.147>>.

Munguia, J., Akande, S. and Dalgarno, K.W., 2014. Compliant flexural behaviour in laser sintered nylon structures: Experimental test and Finite Element Analysis - correlation. *Materials and Design*, [online] 54, pp.652–659. Available at: <<http://dx.doi.org/10.1016/j.matdes.2013.08.088>>.

Nordin, N.M., Buys, Y.F., Anuar, H., Ani, M.H. and Pang, M.M., 2019. Development of conductive polymer composites from PLA/TPU blends filled with graphene nanoplatelets. *Materials Today: Proceedings*, [online] 17, pp.500–507. Available at: <<https://doi.org/10.1016/j.matpr.2019.06.328>>.

Özen, A., Auhl, D., Völlmecke, C., Kiendl, J. and Abali, B.E., 2021. Optimization of manufacturing parameters and tensile specimen geometry for fused deposition modeling (FDM) 3D-printed PETG.

Pandzic, A., Hodzic, D. and Milovanovic, A., 2019. Effect of infill type and density on tensile properties of pla material for fdm process. *Annals of DAAAM and Proceedings of the International DAAAM Symposium*, 30(1), pp.545–554.

Polymerdatabase, 2020. *MOONEY-RIVLIN MODEL*. [online] Polymerdatabase.com. Available at: <[http://polymerdatabase.com/polymerphysics/Mooney-Rivlin Model.html](http://polymerdatabase.com/polymerphysics/Mooney-Rivlin%20Model.html)>.

Rankouhi, B., Javadpour, S., Delfanian, F. and Letcher, T., 2016. Failure Analysis and Mechanical Characterization of 3D Printed ABS With Respect to Layer Thickness and Orientation. *Journal of Failure Analysis and Prevention*, 16(3), pp.467–481.

Rigoussen, A., Raquez, J.M., Dubois, P. and Verge, P., 2019. A dual approach to compatibilize PLA/ABS immiscible blends with epoxidized cardanol derivatives. *European Polymer Journal*, [online] 114(December 2018), pp.118–126. Available at: <<https://doi.org/10.1016/j.eurpolymj.2019.02.017>>.

Sodeifian, G., Ghaseminejad, S. and Yousefi, A.A., 2019. Preparation of polypropylene/short glass fiber composite as Fused Deposition Modeling (FDM) filament. *Results in Physics*, [online] 12(November 2018), pp.205–222. Available at: <<https://doi.org/10.1016/j.rinp.2018.11.065>>.

Sukindar, N.A. Bin, Bin, M.K.A.M.A., Hang Tuah Bin, B.T.B., Binti, C.N.A.J. and Bin, M.I.S.I., 2017. Analysis on the impact process parameters on tensile strength using 3d printer repetier-host software. *ARPN Journal of Engineering and Applied Sciences*, 12(10), pp.3341–3346.

Tanikella, N.G., Wittbrodt, B. and Pearce, J.M., 2017. Tensile strength of commercial polymer materials for fused filament fabrication 3D printing. *Additive Manufacturing*, [online] 15, pp.40–47. Available at: <<http://dx.doi.org/10.1016/j.addma.2017.03.005>>.

Vinyas, M., Athul, S.J., Harursampath, D. and Nguyen Thoi, T., 2019. Mechanical characterization of the Poly lactic acid (PLA) composites prepared through the Fused Deposition Modelling process. *Materials Research Express*, 6(10).

Wang, K., Xie, X., Wang, J., Zhao, A., Peng, Y. and Rao, Y., 2020. Effects of infill characteristics and strain rate on the deformation and failure properties of additively manufactured polyamide-based composite structures. *Results in Physics*, [online] 18(April), p.103346. Available at: <<https://doi.org/10.1016/j.rinp.2020.103346>>.

Wu, H.X., Jiang, S.Q., Cui, H.R. and Cui, J.Y., 2014. Maleic anhydride grafted modified PA6 as compatilizer preparation of PLA/PA6 blend. *Applied Mechanics and Materials*, 590, pp.284–288.

Xiang, D., Zhang, X., Li, Y., Harkin-Jones, E., Zheng, Y., Wang, L., Zhao, C. and Wang, P., 2019. Enhanced performance of 3D printed highly elastic strain sensors of carbon nanotube/thermoplastic polyurethane nanocomposites via non-covalent interactions. *Composites Part B: Engineering*, [online] 176(August), p.107250. Available at: <<https://doi.org/10.1016/j.compositesb.2019.107250>>.

Zhong, W., Li, F., Zhang, Z., Song, L. and Li, Z., 2001. Short fiber reinforced composites for fused deposition modeling. *Materials Science and Engineering A*, 301(2), pp.125–130.

APPENDICES

Appendix A: Result from Finite Element Analysis

Table A-1: Mechanical properties of ABS/TPU

ABS/TPU						
Infill Pattern	Shell Thickness (mm)	Infill Density (%)	Tensile Strength (MPa)	Tensile Modulus (MPa)	Flexural Strength (MPa)	Flexural Modulus (MPa)
Hexagonal	0.4	20	3.0642	156.03	1.091	54.022
		60	2.7485	138.93	0.4487	11.787
		100	17.201	311.48	2.9096	72.425
	0.8	20	15.881	786.4	1.7494	37.133
		60	16.476	300.56	0.45421	13.768
		100	25.112	573.53	2.9088	79.275
	1.2	20	20.606	957.53	1.1628	40.447
		60	13.297	357.36	1.3786	13.624
		100	19.276	740.88	3.3429	100.78
Triangular	0.4	20	7.6858	185.29	1.3695	33.672
		60	2.9304	64.379	0.46019	12.065
		100	17.201	311.48	2.9096	72.425
	0.8	20	13.213	403.52	1.1359	23.474
		60	14.231	123.85	0.50042	13.116
		100	25.112	573.53	2.9088	79.275
	1.2	20	16.314	545.85	0.96271	23.052
		60	5.5912	163.81	0.46968	19.926
		100	19.276	740.88	3.3429	100.78

Table A-2: Mechanical properties of PA6/ABS

PA6/ABS						
Infill Pattern	Shell Thickness (mm)	Infill Density (%)	Tensile Strength (MPa)	Tensile Modulus (MPa)	Flexural Strength (MPa)	Flexural Modulus (MPa)
Hexagonal	0.4	20	21.515	495.23	2.4438	40.736
		60	25.609	93.805	3.5795	77.446
		100	30.52	1101.1	3.4662	75.828
	0.8	20	31.086	285.72	1.8062	34.104
		60	33.406	866.65	2.872	55.098
		100	26.663	863.78	3.121	63.408
	1.2	20	32.16	283.25	1.1517	23.069
		60	34.274	982.01	1.749	33.638
		100	34.941	696.36	1.9258	37.887
Triangular	0.4	20	22.113	771.99	2.2873	63.987
		60	32.329	1263	3.8326	99.7
		100	30.52	1101.1	3.4662	75.828
	0.8	20	31.97	796.8	2.2514	50.481
		60	31.845	1087.7	3.1245	75.254
		100	26.663	863.78	3.121	63.408
	1.2	20	34.014	571.21	1.5493	29.685
		60	35.541	1026.6	2.2094	43.741
		100	34.941	696.36	1.9258	37.887

Table A-3: Mechanical properties of PLA/ABS

PLA/ABS						
Infill Pattern	Shell Thickness (mm)	Infill Density (%)	Tensile Strength (MPa)	Tensile Modulus (MPa)	Flexural Strength (MPa)	Flexural Modulus (MPa)
Hexagonal	0.4	20	14.577	933.34	5.2279	181.01
		60	25.913	1198.5	3.8279	100.99
		100	37.804	1381.7	6.8027	198.13
	0.8	20	27.168	1254.7	4.7001	172.58
		60	25.706	1198	3.162	112.36
		100	38.602	1383.5	6.0566	191.27
	1.2	20	31.224	1310.5	6.0139	150.66
		60	27.964	1250.6	3.5068	80.442
		100	39.66	1407.4	5.4782	152.05
Triangular	0.4	20	22.879	1122.2	3.6151	125.8
		60	31.839	1227.7	4.5198	137.57
		100	37.804	1381.7	6.8027	198.13
	0.8	20	26.15	1249.1	4.2241	129.78
		60	31.865	1243.6	3.8497	110.91
		100	38.602	1383.5	6.0566	191.27
	1.2	20	26.068	1222.3	4.2522	106.83
		60	31.631	1229.3	2.922	87.477
		100	39.66	1407.4	5.4782	152.05

Table A-4: Mechanical properties of PLA/PA6

PLA/PA6						
Infill Pattern	Shell Thickness (mm)	Infill Density (%)	Tensile Strength (MPa)	Tensile Modulus (MPa)	Flexural Strength (MPa)	Flexural Modulus (MPa)
Hexagonal	0.4	20	6.3109	245.85	2.1119	90.757
		60	10.341	212.65	0.96936	24.707
		100	19.274	412.13	3.491	100.47
	0.8	20	18.819	838.28	3.1107	105.9
		60	10.64	357.98	0.73345	36.926
		100	22.838	646.32	3.847	120.31
	1.2	20	24.226	937.15	3.4581	85.012
		60	11.456	410.26	1.7804	46.763
		100	24.424	811.19	4.6646	136.37
Triangular	0.4	20	8.3442	265.29	1.7496	49.679
		60	12.719	149.33	0.88304	22.003
		100	19.274	412.13	3.491	100.47
	0.8	20	12.566	482.16	1.8942	65.658
		60	9.9553	199.39	0.86957	28.714
		100	22.838	646.32	3.847	120.31
	1.2	20	14.22	607.6	2.2685	75.302
		60	7.1001	232.67	1.3429	38.543
		100	24.424	811.19	4.6646	136.37

Table A-5: Mechanical properties of PLA/PETG

PLA/PETG						
Infill Pattern	Shell Thickness (mm)	Infill Density (%)	Tensile Strength (MPa)	Tensile Modulus (MPa)	Flexural Strength (MPa)	Flexural Modulus (MPa)
Hexagonal	0.4	20	18.39	908.17	4.857	177.95
		60	36.512	1159.7	3.1032	107.96
		100	50.745	1280.3	6.2751	178.93
	0.8	20	27.314	1232.8	4.3749	167.38
		60	32.84	1160.6	2.7058	103.83
		100	48.476	1307.8	5.5229	185.52
	1.2	20	31.999	1287.2	5.2833	164.98
		60	34.151	1206.4	3.0685	86.387
		100	46.962	1344.8	4.9853	162.86
Triangular	0.4	20	31.435	1063.8	3.5939	127.39
		60	45.096	1181.3	4.7126	127.89
		100	50.745	1280.3	6.2751	178.93
	0.8	20	31.357	1211.6	3.0912	125.81
		60	43.917	1189	3.5571	94.931
		100	48.476	1307.8	5.5229	185.52
	1.2	20	30.006	1211.1	2.8482	112.8
		60	42.197	1186	2.4213	81.305
		100	46.962	1344.8	4.9853	162.86

Table A-6: Mechanical properties of PLA/TPU

PLA/TPU						
Infill Pattern	Shell Thickness (mm)	Infill Density (%)	Tensile Strength (MPa)	Tensile Modulus (MPa)	Flexural Strength (MPa)	Flexural Modulus (MPa)
Hexagonal	0.4	20	3.2379	164.18	1.1551	57.808
		60	16.77	143.5	0.4611	10.571
		100	18.474	311.16	2.7929	87.43
	0.8	20	18.105	831.5	1.1047	43.06
		60	9.2648	319.11	0.54904	12.341
		100	16.798	583.38	3.0081	113.09
	1.2	20	23.267	997.86	1.2153	47.686
		60	13.956	378.78	0.63512	20.428
		100	30.355	751.46	3.4549	126.28
Triangular	0.4	20	5.8245	196.39	0.94407	37.498
		60	16.963	66.304	0.47394	14.071
		100	18.474	311.16	2.7929	87.43
	0.8	20	9.5334	429.99	0.87624	25.412
		60	6.3664	127.22	0.38864	11.656
		100	16.798	583.38	3.0081	113.09
	1.2	20	16.881	588.86	0.99397	25.077
		60	17.427	169.35	0.57101	16.8
		100	30.355	751.46	3.4549	126.28

Table A-7: Mechanical properties of ABS

ABS						
Infill Pattern	Shell Thickness (mm)	Infill Density (%)	Tensile Strength (MPa)	Tensile Modulus (MPa)	Flexural Strength (MPa)	Flexural Modulus (MPa)
Hexagonal	0.4	20	18.019	1005.3	5.0911	142.22
		60	25.442	1179.4	3.9339	110.89
	0.8	20	22.23	1180.3	4.6198	129.97
		60	24.301	1159.8	3.1565	92.017
		100	36.613	1367	5.8145	150.26
	1.2	20	26.132	1251.6	5.3016	129.38
60		26.088	1216.3	3.3517	68.528	
Triangular	0.4	20	21.759	1101.3	3.5685	115.53
		60	31.398	1212.4	4.2843	125.63
	0.8	20	24.163	1222.4	3.4596	106.02
		60	30.766	1220.9	3.7119	93.644
	1.2	20	23.809	1180.8	3.074	92.8
		60	30.294	1200.5	2.9301	67.536

Table A-8: Mechanical properties of PA6

PA6						
Infill Pattern	Shell Thickness (mm)	Infill Density (%)	Tensile Strength (MPa)	Tensile Modulus (MPa)	Flexural Strength (MPa)	Flexural Modulus (MPa)
Hexagonal	0.4	20	20.153	82.656	0.47555	10.686
		60	25.6	95.697	0.43321	7.3037
	0.8	20	25.898	92.654	0.451	9.7238
		60	27.115	92.921	0.28947	6.8685
		100	34.429	116.12	0.64595	11.776
	1.2	20	28.688	98.294	0.53089	10.255
60		28.323	97.443	0.34391	5.2721	
Triangular	0.4	20	21.157	86.691	0.50057	8.6905
		60	28.689	99.43	0.50148	9.4886
	0.8	20	25.753	97.272	0.41202	8.1597
		60	29.427	99.565	0.37844	7.2968
	1.2	20	26.871	94.88	0.39021	7.2376
		60	29.783	98.781	0.26831	5.3594

Table A-9: Mechanical properties of PETG

PETG						
Infill Pattern	Shell Thickness (mm)	Infill Density (%)	Tensile Strength (MPa)	Tensile Modulus (MPa)	Flexural Strength (MPa)	Flexural Modulus (MPa)
Hexagonal	0.4	20	19.693	843.49	4.3793	143.64
		60	36.924	1121.3	5.9551	172.47
	0.8	20	35.744	1091	5.8466	142.48
		60	34.347	1083.9	7.2936	194.468
		100	53.479	1408.5	7.9682	224.3
	1.2	20	40.402	1137.8	6.2458	138.87
60		41.466	1200.5	8.956	174.921	
Triangular	0.4	20	31.435	1063.8	3.4091	116.44
		60	45.411	1158.3	4.9089	150.69
	0.8	20	34.918	771.97	5.5017	199.365
		60	44.357	1150.6	7.1005	90.782
	1.2	20	35.083	1094.7	3.7932	94.131
		60	43.472	1134.5	3.9932	155.218

Table A-10: Mechanical properties of PLA

PLA						
Infill Pattern	Shell Thickness (mm)	Infill Density (%)	Tensile Strength (MPa)	Tensile Modulus (MPa)	Flexural Strength (MPa)	Flexural Modulus (MPa)
Hexagonal	0.4	20	20.732	532.02	3.3858	167.94
		60	28.701	1301.4	5.6236	210.55
	0.8	20	31.455	1064.6	4.434	227.08
		60	31.247	1386.5	6.4444	239.44
		100	41.46	1763	6.2282	198.29
	1.2	20	30.891	1347.4	5.4287	170.92
60		32.051	1376.6	5.4293	92.402	
Triangular	0.4	20	24.621	590.18	4.3574	141.93
		60	34.662	1313.3	4.7516	237.56
	0.8	20	27.812	965.44	4.6458	237
		60	34.839	1301.1	6.3662	288.87
	1.2	20	31.156	1422.8	4.0511	192.23
		60	33.721	1280.6	5.1031	248.3

Table A-11: Mechanical properties of TPU

TPU						
Infill Pattern	Shell Thickness (mm)	Infill Density (%)	Tensile Strength (MPa)	Tensile Modulus (MPa)	Flexural Strength (MPa)	Flexural Modulus (MPa)
Hexagonal	0.4	20	3.2445	7.7127	0.0387	1.099
		60	4.1505	8.6213	0.0359	0.6882
	0.8	20	3.5817	8.4251	0.0497	1.0497
		60	3.991	8.2308	0.0217	0.6527
		100	5.3635	10.205	0.0532	1.1318
	1.2	20	4.138	8.9435	0.0519	1.0497
60		4.2967	8.7622	0.034	0.5789	
Triangular	0.4	20	3.5991	8.2039	0.0374	0.7633
		60	4.6547	9.3017	0.0405	0.8449
	0.8	20	3.9798	8.6186	0.0384	0.7987
		60	4.5245	9.2205	0.0295	0.6621
	1.2	20	4.0164	8.025	0.045	0.6797
		60	4.4827	9.0527	0.0317	0.4905

Appendix B: Comparison of Finite Element Analysis Result and Experimental Result

Table B-1: Tensile strength comparison of PETG

	Experimental Result (MPa)	Simulation Result (MPa)	Error margin (%)
100% infill 0.8mm shell	53.6065	53.479	0.24
Hex 20% infill 0.4mm shell	20.3163	19.693	3.07
Hex 60% infill 0.4mm shell	38.0137	36.924	2.87
Hex 20% infill 0.8mm shell	37.4394	35.744	4.53
Hex 60% infill 0.8mm shell	34.6858	34.347	0.98
Tri 20% infill 0.4mm shell	17.0124	31.435	45.88
Tri 60% infill 0.4mm shell	24.2673	44.48	45.44
Tri 20% infill 0.8mm shell	33.77934	34.918	3.37
Tri 60% infill 0.8mm shell	40.7945	44.357	8.73

Table B-2: Tensile modulus comparison of PETG

	Experimental Result (MPa)	Simulation Result (MPa)	Error margin (%)
100% infill 0.8mm shell	1400	1408.5	0.61
Hex 20% infill 0.4mm shell	659.21	843.49	27.95
Hex 60% infill 0.4mm shell	1104.4	1121.3	1.53
Hex 20% infill 0.8mm shell	974.09	1091	12.00
Hex 60% infill 0.8mm shell	1268.5	1083.9	14.55
Tri 20% infill 0.4mm shell	679.47	1063.8	56.56
Tri 60% infill 0.4mm shell	854.61	669.88	21.62
Tri 20% infill 0.8mm shell	985.56	1122.1	13.85
Tri 60% infill 0.8mm shell	1153.2	1150.6	0.23

Table B-3: Tensile strength comparison of PLA

	Experimental Result (MPa)	Simulation Result (MPa)	Error margin (%)
100% infill 0.8mm shell	41.5499	41.46	0.22
Hex 20% infill 0.4mm shell	21.8045	20.732	4.92
Hex 60% infill 0.4mm shell	28.0288	28.701	2.40
Hex 20% infill 0.8mm shell	30.6553	31.455	2.61
Hex 60% infill 0.8mm shell	34.1931	31.247	8.62
Tri 20% infill 0.4mm shell	17.8379	24.482	37.25
Tri 60% infill 0.4mm shell	23.1164	32.662	41.29
Tri 20% infill 0.8mm shell	28.9974	27.812	4.09
Tri 60% infill 0.8mm shell	33.1557	34.839	5.08

Table B-4: Tensile modulus comparison of PLA

	Experimental Result (MPa)	Simulation Result (MPa)	Error margin (%)
100% infill 0.8mm shell	1736.1	1763	1.55
Hex 20% infill 0.4mm shell	718.08	532.02	25.91
Hex 60% infill 0.4mm shell	1217.3	1301.4	6.91
Hex 20% infill 0.8mm shell	1106.2	1064.6	3.76
Hex 60% infill 0.8mm shell	1290.2	1386.5	7.46
Tri 20% infill 0.4mm shell	729.87	685.7	6.05
Tri 60% infill 0.4mm shell	1049.8	1313.3	25.10
Tri 20% infill 0.8mm shell	1057.1	965.44	8.67
Tri 60% infill 0.8mm shell	1361	1301.1	4.40

Table B-5: Flexural strength comparison of PETG

	Experimental Result (MPa)	Simulation Result (MPa)	Error margin (%)
100% infill 0.8mm shell	7.9130	7.9682	0.70
Hex 20% infill 0.4mm shell	3.9051	4.3793	12.14
Hex 60% infill 0.4mm shell	5.9779	5.9551	0.38
Hex 20% infill 0.8mm shell	6.0469	5.8466	3.31
Hex 60% infill 0.8mm shell	7.0937	7.2936	2.82
Tri 20% infill 0.4mm shell	2.8543	3.4091	19.44
Tri 60% infill 0.4mm shell	4.9667	4.9089	1.16
Tri 20% infill 0.8mm shell	5.5968	5.5017	1.70
Tri 60% infill 0.8mm shell	7.0811	7.1005	0.27

Table B-6: Flexural modulus comparison of PETG

	Experimental Result (MPa)	Simulation Result (MPa)	Error margin (%)
100% infill 0.8mm shell	231.64	224.3	3.17
Hex 20% infill 0.4mm shell	139.51	143.64	2.96
Hex 60% infill 0.4mm shell	183.6	172.47	6.06
Hex 20% infill 0.8mm shell	181.05	142.48	21.30
Hex 60% infill 0.8mm shell	206.92	194.468	6.02
Tri 20% infill 0.4mm shell	122.49	116.44	4.94
Tri 60% infill 0.4mm shell	172.21	150.69	12.50
Tri 20% infill 0.8mm shell	180.51	199.365	10.45
Tri 60% infill 0.8mm shell	255.76	290.782	13.69

Table B-7: Flexural strength comparison of PLA

	Experimental Result (MPa)	Simulation Result (MPa)	Error margin (%)
100% infill 0.8mm shell	5.5920	6.23	11.41
Hex 20% infill 0.4mm shell	3.7393	3.3858	9.45
Hex 60% infill 0.4mm shell	5.4294	5.6236	3.58
Hex 20% infill 0.8mm shell	4.3652	4.434	1.58
Hex 60% infill 0.8mm shell	5.8763	6.444	9.66
Tri 20% infill 0.4mm shell	3.7829	4.3574	15.19
Tri 60% infill 0.4mm shell	4.6968	4.7516	1.17
Tri 20% infill 0.8mm shell	4.9250	4.6458	5.67
Tri 60% infill 0.8mm shell	6.3381	6.3662	0.44

Table B-8: Flexural modulus comparison of PLA

	Experimental Result (MPa)	Simulation Result (MPa)	Error margin (%)
100% infill 0.8mm shell	185.59	198.29	6.84
Hex 20% infill 0.4mm shell	166.66	167.94	0.77
Hex 60% infill 0.4mm shell	212.76	210.55	1.04
Hex 20% infill 0.8mm shell	204.99	227.08	10.78
Hex 60% infill 0.8mm shell	225.24	239.44	6.30
Tri 20% infill 0.4mm shell	160.31	141.93	11.47
Tri 60% infill 0.4mm shell	215.04	237.56	10.47
Tri 20% infill 0.8mm shell	236.13	237	0.37
Tri 60% infill 0.8mm shell	265.82	288.87	8.67



Figure B-1: The composites sample fabricated

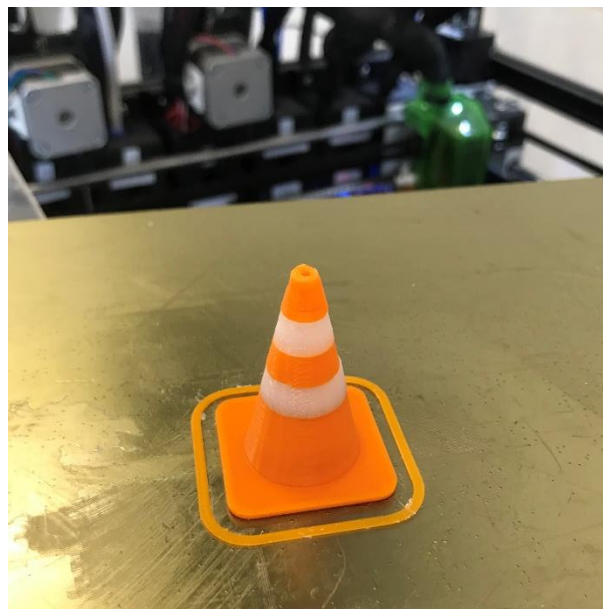


Figure B- 2: Cone shape printed using two extruders on multitools 3D printer



Figure B- 3: Multitools 3D printer used for sample fabrication

Procedure to Operate the Multitools 3D Printer

This section clearly explains the detailed information on the operating procedure and calibration process involved in the Multitools 3D printer operation. Figure B-4 shows the flow chart of how to 3D print the test samples. After exporting the generated G-code into a USB drive, insert the USB drive into the USB port of the printer.

Firstly, heat the extruder to the melting temperature of the filament material before inserting the filament. Proceed with inserting filament into the extruder accordingly when the temperature is set. The filament has to be inserted into the extruder according to the filament arrangement set in PrusaSlicer, as shown in Figure B-5. After inserting the filament, an extrusion of 100 mm was done to purge the leftover material in the nozzle from the previous print. If the extruder does not get rid of the material, check the temperature of the extruder hot-end and the movement of the extruder motor. Then, put the filament back in.

After finding out that the extruder can purge the filament material smoothly, proceed with the 3D printing process by choosing the file printed on the USB drive. When starting printing, observe the distance between the nozzle and the bed to ensure it is as per the settings in the Prusaslicer. If the distance between the nozzle and the bed is too far or close, increase or

decrease baby steps to the desired length. Moreover, when printing with two or more extruders, X and Y-offset also have to be set. If the X or Y offset of the extruder is not set correctly, there will be a gap when printing with two or more extruders, as shown in Figure B-6. Besides, suppose the Z-offset of the extruder is not set correctly. In that case, the distance of the nozzle to the bed or previous layer will be either too close or too far, which will significantly affect the print quality and affect the adhesion between the layers of different materials.

The calibration process involves setting the hot-end offset. The multitool 3D printer has six hot-end, so there must be an offset when printing with different hot-end. This calibration process is involved in making sure the infill and shell of the 3D print test samples stick to each other when printing with different hot-end for infill material and shell material. The hot-end offset can be set through the screen on the multitools 3D printer. To check the X and Y-offset, first, initialize tool T0 and use g-code `G1 X125 Y150 Z3 F4000` to move the extruder T0 to position 125 on the x-axis, 150 on the y-axis, and three on the z-axis with a speed of 4000 mm/min. Then proceed by placing a piece of paper with an "X" mark on it right under the nozzle head to mark the position. Then return to T0, grab the next extruder T1, and use the same g-code `G1 X125 Y150 Z3 F4000` to position the extruder T1. To calculate the offset distance:

1. Use the move function with a precision of 0.01 mm.
2. Proceed with checking the current offset value by using the M218 code in the terminal, subtracting or adding the distance from the offset to the current offset value according to the condition.
3. Proceed by inserting `M218 T1 X0.2 Y0 Z0` in the terminal, which indicates T1 extruder X-offset of 0.2mm, and lastly, inserts the M500 code to save the setting in the printer.
4. For the Z-offset setting, grab the extruder and use the same g-code to move the extruder.
5. Place a piece of paper between the nozzle and the bed, and pull and push the paper while moving up the print bed until the paper is touching the nozzle and bed.

6. Proceed with grabbing the other extruder to calculate the offset value and proceed with the same step as setting the X and Y offset.

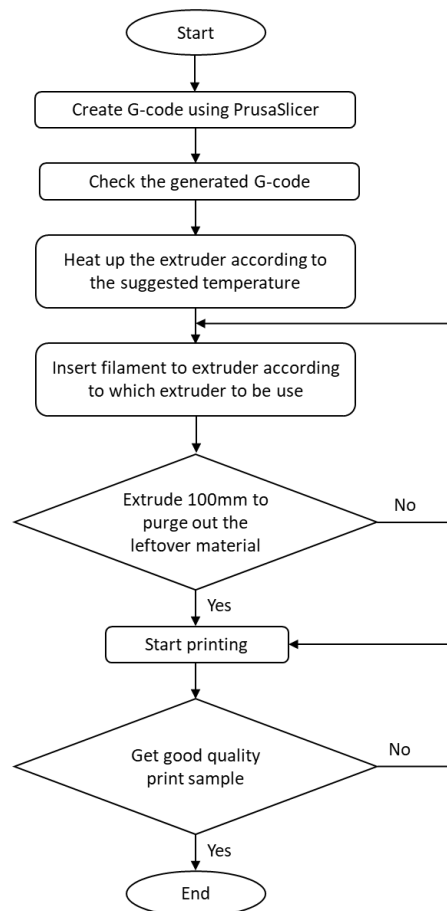


Figure B-4: 3D printing operating procedure flow chart

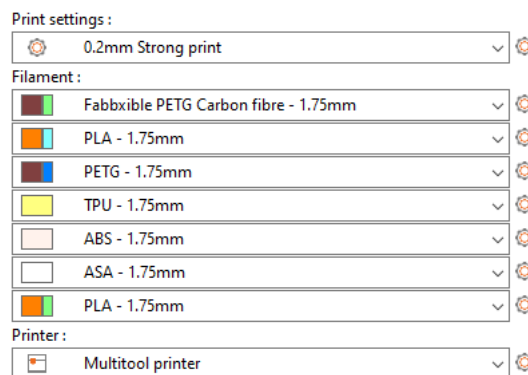


Figure B-5: The filament arrangement in PrusaSlicer as set

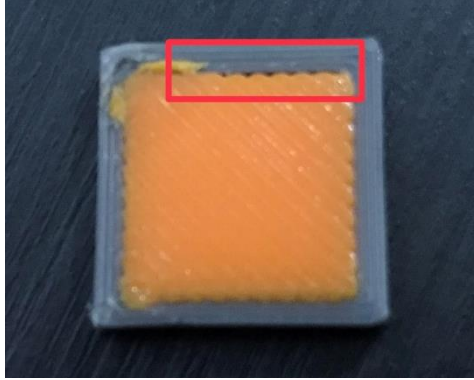


Figure B-6: Offset when printing with different extruder